LUND UNIVERSITY

Verification of Dose Calculation Algorithms in Treatment Planning Systems for External Radiation Therapy: A Monte Carlo Approach

Wieslander, Elinore

2006

Total number of authors:
1

Verification of Dose Calculation Algorithms in Treatment Planning Systems for External Radiation Therapy

A Monte Carlo Approach

Elinore Wieslander

Medical Radiation Physics
Department of Clinical Sciences, Lund
Lund University, Sweden
2006

LUND UNIVERSITY

Abstract

This thesis presents a new verification concept, *the virtual accelerator*, for dose calculation algorithms used in treatment planning systems (TPSs) for external beam radiotherapy. The algorithm input data required to implement a treatment unit in the TPS are generated by Monte Carlo simulations as are the beam reference data needed for the subsequent evaluation of the dose calculation algorithm. The virtual accelerator and its corresponding unit in the TPS can thus be used for comprehensive verification of dose calculation algorithms in the TPS.

The virtual accelerator concept provides a new means of verifying dose calculation algorithms in TPSs. Properties that are difficult or even impossible to assess using conventional measurements can be studied. Problems associated with conventional measurements, e.g., detector limitations and accelerator stability, can be circumvented. The flexibility of the virtual accelerator is high since additional beam reference data can be acquired without compromising the consistency of the data.

The feasibility of the virtual accelerator concept has been demonstrated by the successful implementation of a virtual photon accelerator and a virtual electron accelerator in commercial TPSs. The success of the implementations was determined by the ability of the dose calculation algorithms to reproduce the algorithm input data, and in most cases the agreement was within ±2%.

The advantages and usefulness of the virtual photon accelerator have been illustrated in a mediastinum and a hip-prostheses-like geometry. The ability of the virtual photon accelerator to generate both total dose and the primary and phantom-scattered components was used to study the performance of two dose calculation algorithms in the presence of metallic implants.

The virtual electron accelerator has been used to study the performance in homogeneous and inhomogeneous phantoms. Studies of the beam model and the handling of patient-specific inserts in the dose calculation algorithm were possible due to the ability of the virtual accelerator to separate the total dose into beam model components.

Another advantage of the virtual accelerator that has been utilized for both photons and electrons is the possibility of evaluating the accuracy achievable in anthropomorphic phantoms based on patient X-ray computed tomography data. This feature has been used for photon algorithms in the case of tangential breast treatment and for the electron algorithm in the cases of nose, parotid gland, thorax wall and spinal cord treatment. For the electron cases, an elliptical γ-evaluation was performed in three dimensions. For the 0.02 Gy/2 mm criteria 92% of the volume receiving more than 0.85 Gy per 100 monitor units (MU) has γ-values less than one in the worst case. The corresponding value for the volume receiving more than 0.10 Gy/100 MU is 98%.

Key words: radiotherapy, treatment planning system, dose calculation algorithm, verification, Monte Carlo calculation, electron beam, photon beam

List of original papers

This thesis is based on studies reported in the following papers, which are referred to in the text by their roman numerals. The papers are appended at the end of the thesis.

    I.   Wieslander E and Knöös T: A virtual linear accelerator for verification of treatment planning systems
            Phys. Med. Biol. **45** 2887-2896, 2000

    II.   Wieslander E and Knöös T: Dose perturbation in the presence of metallic implants: treatment planning system versus Monte Carlo simulations
            Phys. Med. Biol. **48** 3295-3305, 2003

    III.   Wieslander E and Knöös T: A virtual-accelerator-based verification of a Monte Carlo dose calculation algorithm for electron beam treatment planning in homogeneous phantoms
            Submitted to *Phys. Med. Biol.*, 2005

    IV.   Wieslander E and Knöös T: A virtual-accelerator-based verification of a Monte Carlo dose calculation algorithm for electron beam treatment planning in clinical situations
            Submitted to *Phys. Med. Biol.*, 2005

Reports have been presented at the following international meetings:

i   The XIIIth International Conference on the Use of Computers in Radiation Therapy, Heidelberg, Germany, 2000 (Wieslander E and Knöös T, A virtual linear accelerator for verification of treatment planning systems In: Proceedings Schlegel W and Bortfeld T Eds. 446-448 (Heidelberg: Springer-Verlag))

ii   The 6th Biennial ESTRO Meeting, Seville, Spain, 2001 (Wieslander E, Sheikh-Bagheri D, Weber L, Ahnesjö A and Knöös T, Monte Carlo verification of a multi-source model used in a treatment planning system *Radiother. Oncol.* **61** (suppl. 1) S101)

iii   The 21st Annual ESTRO Meeting, Prague, Czech Republic, 2002 (Wieslander E and Knöös T, Dose perturbations in the presence of metallic prosthesis: TPS vs. Monte Carlo simulations *Radiother. Oncol.* **64** (suppl. 1) S36)

iv   The 23rd Annual ESTRO Meeting, Amsterdam, Netherlands, 2004 (Wieslander E, Traneus E and Knöös T, A virtual electron accelerator, based on Monte Carlo, for verification of a commercial Monte Carlo electron treatment planning system *Radiother. Oncol.* **73** (suppl. 1) S375)

v   The 14th International Conference of Medical Physics, Nuremberg, Germany, 2005 (Wieslander E and Knöös T, A virtual accelerator for verification of electron dose calculations in a treatment planning system In: Proceedings Kalender W, Hahn E G and Schulte A M Eds. *Biomedizinische Technik* 50 (Suppl 1) 881-882 (Berlin: Fachverlag Schiele & Schön GmbH))

vi   The 8th Biennial ESTRO Meeting, Lisbon, Portugal, 2005 (Wieslander E and Knöös T, A virtual accelerator for validation of an electron dose calculation module in the presence of inhomogeneities *Radiother. Oncol.* **76** (suppl. 2) S152)

Contents

Abbreviations

1D	One-dimensional
2D	Two-dimensional
3D	Three-dimensional
CC	Collapsed cone
CT	X-ray computed tomography
dta	Distance to agreement
EGS	Electron-Gamma-Shower
EPS	Exit phase space
HU	Hounsfield units
IC	Ionization chamber
MC	Monte Carlo
MR	Magnetic resonance
MU	Monitor unit
OMP	Oncentra MasterPlan
PB	Pencil beam
PET	Positron-emission tomography
PSF	Point spread function
SD	Standard deviation
SPS	Source phase space
SSD	Source-skin distance
TLD	Thermoluminescent dosimeter
TPS	Treatment planning system
QA	Quality assurance

1 Preface

1.1 Introduction

Radiotherapy is an important modality for both curative and palliative treatment of cancer. It can be used either in combination with, e.g., surgery and/or chemotherapy or as the sole treatment modality. The proportion of cancer patients that would benefit from external beam radiation therapy, at least once during their illness, has been calculated to be 52% (Delaney *et al* 2005). It has been estimated that about half of the cancer cases in Sweden receive radiotherapy (Ringborg *et al* 2003).

The aim of radiotherapy is to deliver a very accurate absorbed dose to a well-defined target volume with minimal absorbed dose to the surrounding normal tissue, especially highly radiosensitive organs. The uncertainty in the delivered dose to the patient should be less than 3-5% (1 standard deviation, SD) (ICRU 1976, Mijnheer *et al* 1987, Brahme *et al* 1988, Wambersie 2001). However, it has been recognized that in some cases, e.g. in palliative treatment, higher uncertainties are acceptable (Wambersie 2001). Precise dose delivery, both geometrically and dosimetrically, is therefore crucial for the successful outcome of the treatment.

The geometrical issues associated with dose delivery and patient positioning, inter- or intra-fractional, can today be managed due to the introduction of advanced imaging and delivery techniques allowing high conformity of the delivered dose to the target volume (Mackie *et al* 2003, Mageras and Yorke 2004, Herman 2005, Jaffray 2005, Webb 2005). However, large geometrical uncertainties are still associated with delineation of the target volume and organs at risk (Leunens *et al* 1993, Giraud *et al* 2002). The accuracy in volume delineation can today be improved by complementing routine X-ray computed tomography (CT) with a variety of imaging modalities. Both anatomical and functional modalities, such as positron-emission tomography (PET), magnetic resonance (MR) and single-photon-emission computed tomography are used (Paulino *et al* 2003, Rasch *et al* 2005).

The dosimetric issues are associated with the accuracy of the commissioning process of radiation beams in homogeneous water phantoms, the subsequent stability of the treatment delivery equipment, and the in-patient dose calculation. Recommendations regarding beam calibration under reference conditions (i.e. absorbed dose determination at a single point in a well-defined geometry) and relative dosimetry in homogeneous water phantoms have been given by several organisations (e.g. AAPM 1991, AAPM 1999, IAEA 2000, IPEM 2003). The in-patient dose calculation is performed with dedicated computer-based treatment planning systems (TPSs) that model the dose, based on input data acquired in simple homogeneous geometries.

Monte Carlo (MC) simulations are considered to be the most accurate method available for particle transport and dose calculations in radiotherapy (Rogers and Bielajew 1990, Mackie 1990, Andreo 1991, Ma and Jiang 1999, Rogers 2002, Verhaegen and Seuntjens 2003). Some MC-based algorithms for electron beam treatment planning are commercially available, but the majority of the photon algorithms in commercial TPSs are still based on analytical models of varying complexity. Irrespective of the type of the algorithm, MC or analytical, the user must be aware of its inherent limitations. To achieve an uncertainty of less than 3-5% (1 SD) in the dose delivered to the patient all the uncertainties in the radiotherapy chain must be minimized, including those associated with treatment planning. The validation of dose calculation algorithms in TPSs is commonly performed by comparisons with measured data. The reliability of measured data sets is dependent on the stability of the accelerator, e.g., energy, output, flatness, and symmetry which may vary in time and can only partly be controlled. Other possible limitations on measurements are related to the choice of detector and experimental set-up, which may restrict the number of comparison points and introduce dosimetric problems.

This work presents a MC approach, *a virtual accelerator*, for use in the verification of dose calculation algorithms in TPSs. This approach circumvents problems associated with conventional verification procedures, and enables studies of properties that are difficult or impossible to assess from measured data.

1.2 Aims of the work

The overall aim of this work was to develop a novel verification concept, a *virtual accelerator*, for dose calculation algorithms used in external beam radiotherapy. The virtual accelerator is based on Monte Carlo simulations of both algorithm input data[1] and beam reference data[2]. By introducing the virtual accelerator into the verification of dose calculation algorithms, problems associated with conventional measurements can be avoided. Properties that are impossible to measure can be studied and dose distributions in geometries where it is impossible to perform measurements can be evaluated.

The first aim was to demonstrate the concept of the virtual accelerator. The feasibility of implementing a virtual accelerator in treatment planning systems for both photons and electrons is described in Papers I and III.

---

[1] Algorithm input data refers to the data required for implementation of the treatment unit in the TPS (IAEA 2004).
[2] Beam reference data are data measured by the user to evaluate the quality of the dose calculations (IAEA 2004).

The second aim was to demonstrate the usefulness and the advantages of the virtual accelerator and to investigate the accuracy achievable in a number of situations using three model-based dose calculation algorithms, two for photons and one for electrons.

For photon beams a pencil beam-based algorithm was evaluated:
- in a mediastinum geometry (Paper I) and
- in the presence of metallic implants (Paper II).

A point spread function-based algorithm was evaluated:
- in the presence of metallic implants (Paper II).

For electron beams a MC-based algorithm was evaluated:
- in homogeneous water phantoms (Paper III),
- in the presence of air and bone inhomogeneities (Paper IV) and
- in anthropomorphic phantoms (Paper IV).

1.3   Outline of the thesis

Following this introductory chapter, Chapter 2 discusses some of the issues related to the accuracy and uncertainty in external beam radiotherapy. Chapter 3 gives a short introduction to the MC method and the advantages of MC methods in the verification of dose calculation algorithms in TPSs are discussed. The virtual accelerator concept is introduced and the virtual accelerators for photon and electron beams used in this study are described. A brief overview of the dose calculation algorithms for photons and electrons is given in Chapter 4, as well as aspects regarding their performance in homogeneous and inhomogeneous geometries. The conclusions and suggestions for future work are presented in Chapters 5 and 6.

2 Accuracy and uncertainty considerations in external radiation therapy

An essential tool in the radiation therapy process is the three-dimensional (3D) treatment planning system. A typical TPS consists of the following components.

- Anatomy modules in which images from various modalities (e.g. CT, MR, PET) are used to outline target volumes and organs at risk. The multimodality aspect is facilitated by co-registration of image sets.
- A beam set-up/optimization module in which the optimal beam configuration for either conformal or intensity-modulated radio-therapy is determined.
- A dose calculation module in which the dose to the patient for a specific treatment set-up is calculated based on information from CT images.
- A dose evaluation module in which the pros and cons of several treatment set-ups can be assessed and visualized in order to facilitate decisions regarding the optimal treatment for each patient.
- Finally, a documentation module in which information about the treatment can be documented and exported.

The acceptance test, the commissioning (i.e. preparing a TPS for clinical use), and the quality assurance (QA) of a TPS are complex tasks. Many comprehensive, international and national reports have addressed these issues, regarding both dosimetric and non-dosimetric properties (Dahlin *et al* 1983, Brahme *et al* 1988, Van Dyk *et al* 1993, IPEMB 1996, SGSMP 1997, AAPM 1998, IPEM 1999, IAEA 2004, ESTRO 2004, NCS 2005). The user should be aware that the vendor can not guarantee systems without deficiencies, and that all possible sources of error can never be tested. Therefore, it is common to test the TPS over the range of its intended clinical use, which should be borne in mind when new treatment techniques are implemented in the clinic.

During the commissioning of the dose calculation algorithms, and in the subsequent QA, different types of reference data sets are used. The following data sets have been identified in the IAEA[3] report TRS 430 (IAEA 2004):

- *algorithm input data:* data required for beam parameterization, i.e., implementation of the treatment unit in the TPS,
- *beam reference data:* data measured by the user to evaluate the quality of the dose calculations,
- *benchmark data:* data for generic beams published in the literature or arbitrary self-consistent data, and
- *QA reference data:* data used for future QA.

This nomenclature has been adopted in this thesis and in Papers III and IV. Papers I and II were published before these definitions had been established.

---

[3] International Atomic Energy Agency

2.1 Accuracy requirements in radiation therapy

Normal tissue and tumours respond differently to radiation and the tolerance of normal tissue often limits the dose that can be administered to the target volume. The relationship between the absorbed dose and the associated biological effect can be described by dose-response curves. These curves have a sigmoid shape for both tumours and normal tissue, and the curves are in general steeper for normal tissue. It has been concluded from clinical observations that a difference of 7-10% in absorbed dose can result in detectable tumour and normal tissue reactions (ICRU 1976, Dutreix 1984, Mijnheer *et al* 1987, Wambersie 2001).

Based on dose-response curves Mijnheer *et al* (1987) proposed an accuracy requirement in the absorbed dose delivered to the patient of 3.5% (1 SD). Depending on the steepness of the dose-response curves larger values can be accepted in some cases, while in others an even smaller value is desirable.

Brahme *et al* (1988) recommend a tolerance of 3% (1 SD) in the accuracy of delivered absorbed dose to the patient. They also proposed an action level of 5% (1 SD) above which it is recommended to work seriously to improve the accuracy in the delivered dose.

Wambersie (2001) reports similar requirements to Mijnheer *et al* (1987), i.e., an accuracy of 3.5% (1 SD). Wambersie (2001) also states that higher uncertainties may be inevitable due to other uncertainties such as treatment planning and dose determination under non-reference conditions.

Based on clinical studies, the International Commission on Radiation Units and Measurements (ICRU 1976) concluded that evidence from some tumours indicates that an accuracy of 5% in delivered absorbed dose to the target volume is required when eradication of the tumour is the aim. Smaller limits, such as 2%, were proposed by some clinicians, but this was considered at the time (1976) to be virtually unachievable.

To meet the high demand on the accuracy of the absorbed dose delivered to the patient, obviously the uncertainties in all parts of the radiation therapy chain must be minimized.

2.2 Uncertainties in the radiation therapy chain

One way of determining the accuracy required in the dose calculation alone is to identify and quantify the uncertainties associated with the dose delivery chain (Johansson 1982, Mijnheer *et al* 1987, Brahme *et al* 1988, Ahnesjö 1991, Ahnesjö and Aspradakis 1999, AAPM 2004). Table 1 summarizes data adopted from Ahnesjö and Aspradakis (1999) for photon beams, where the uncertainty regarding the dose at the calibration point is according to IAEA (2000). The currently achievable accuracy is presented together with an estimate of future uncertainties. The uncertainties stated are valid when a comprehensive QA programme has been implemented, and larger errors should be expected for more complex treatment techniques. The effect on the overall uncertainty of different levels of accuracy in the dose calculation is shown. The combined

Table 1. Estimates of uncertainty (in terms of 1 SD) in absorbed dose to the patient for the complete treatment procedure using photon beams. Adopted from Ahnesjö and Aspradakis (1999) and modified according to IAEA (2000).

Source of uncertainty	Uncertainty in % (1 SD)	
	Present	Future
Dose determination at the calibration point	1.5*	1.0
Additional uncertainty for other points	1.1	0.5
Beam monitor stability	1.0	0.5
Beam flatness	1.5	0.8
Patient data	1.5	1.0
Beam and patient set-up	2.5	1.6
Overall excluding dose calculation	3.9	2.4
Dose calculation	1.0/2.0/3.0/4.0/5.0	1.0/2.0/3.0
Overall	4.0/4.4/4.9/5.6/6.3	2.6/3.1/3.8

* According to IAEA 2000

uncertainty, excluding that in the dose calculation, is currently greater than the 3.0-3.5% standard deviation limit for the absorbed dose delivered to the patient. To be able to achieve the accuracy goal the uncertainty must be minimized, not only in the dose calculation stage but throughout the whole delivery chain.

Based on the data in Table 1 and the assumption that the accuracy in the dose delivered to the patient should be better than 3.0-3.5%, the ultimate future goal for dose calculation accuracy should be 1.0-2.0% (Ahnesjö 1991, Ahnesjö and Aspradakis 1999, AAPM 2004). This is in accordance with the 2.0% or 2.0 mm in high dose gradients stated in ICRU 42 (ICRU 1987) regarding the accuracy of computer-produced dose distributions. ICRU has here adopted the shift of isodose lines that is often proposed as an alternative in regions with high dose gradients (>3% change in dose per mm).

Uncertainties in the TPS dose calculation arise from the uncertainty in the original measured algorithm input data, the transfer of data to the TPS and the way in which the data are used. The algorithm input data can be influenced by accelerator stability, the resolution and sensitivity of the detectors, and the quality of the data preparation and analysis. Uncertainties associated with the calculation algorithm itself can arise from poor modelling of the physics involved, lack of appropriate supporting information, inappropriate approximations, poor parameterization, too coarse a calculation grid size, and other limitations associated with either the basic algorithm or its use (AAPM 1998). The beam reference data are associated with the same uncertainties as the algorithm input data.

The uncertainties in the dose delivery chain for high-energy electrons are similar to those for high-energy photons (Brahme *et al* 1988, IAEA 2000). Hence, the accuracy of dose calculation algorithms for electrons should be of

the same order as for photons. In the past this has not been practically achievable due to limitations in the dose calculation algorithms used (Van Dyk *et al* 1993, Ding *et al* 1999, Paper IV). However, the new MC-based electron algorithms that are becoming commercially available have the potential to decrease the uncertainties in electron treatment planning.

2.3   Acceptance criteria for accuracy in TPS dose calculations

The level of accuracy required for radiotherapy is based on radiobiological issues. Thus, the accuracy should ultimately be independent of the complexity of the treatment. However, since an increasing complexity in beam set-up adds larger uncertainties to the dose calculations, a wider criterion may, due to practical reasons, be accepted.

Recommendations regarding the accuracy required or achievable, i.e., the acceptance criteria, for dose calculations have been proposed by several authors (ICRU 1987, McCullough and Krueger 1980, Brahme *et al* 1988, Van Dyk *et al* 1993, SGSMP 1997, Venselaar *et al* 2001, NCS 2005). Some of them are summarized in Tables 2 and 3. A common feature of all the recommendations is that the acceptance criteria are often differentiated into low/high dose gradients and low/high dose regions as well as the level of complexity (inhomogeneities, beam modulation etc.).

The acceptance criteria are often expressed as a combination of dose deviation in low-dose-gradient regions and a geometrical concept, distance-to-agreement (dta), in high-dose-gradient regions. The dta is the distance between a reference data point and the nearest point in the calculated distribution with the same dose value. The reason for this is that the dose deviation concept is very sensitive in high dose gradients, where a small displacement results in a large deviation. The opposite is valid for the dta concept.

In Paper III, where the accuracy of a MC-based dose calculation algorithm for electron beams in homogeneous water phantoms is presented, the 2%/2 mm criteria were used. Both 2%/2 mm and 3%/3 mm were used in the study described in Paper IV, in which the performance of the MC-based dose calculation algorithm was studied in clinical situations.

The use of differentiated criteria based on the characteristics of different structures within the patient, i.e., highly dose-sensitive normal tissue in close proximity to the targeted volume, has also been proposed (Low and Dempsey 2003, Bakai *et al* 2003).

Table 2. Summary of acceptance criteria for dose calculation algorithms for both photon and electron beams.

Conditions	Criterion		Reference
	photons	electrons	
Homogeneous calc. (no blocking)			Van Dyk *et al* (1993)[a]
Central ray data	2%	2%	
High dose / low dose gradient	3%	4%	
High dose gradients (>30%/cm)	4 mm	4 mm	
Low dose[b] / low dose gradient	3%	4%	
Inhomogeneity correction			
1 Central ray (electron equilibrium)	3%	5%	
Complex cases			
1 High dose / low dose gradient	4%	7%	
2 High dose gradients (>30%/cm)	4 mm	5 mm	
3 Low dose[b] / low dose gradient	3%	5%	
Low dose gradient	3%	---	Brahme *et al* (1988)
High dose gradient	3 mm	---	
Low dose gradient IC/TLD[c]	3/4%	---	McCullough and Krueger (1980)
High dose gradient IC/TLD[c]	4/4 mm	---	
Low dose gradient	2%	2%	ICRU (1987)
High dose gradient	2 mm	2 mm	

[a] Percentages are defined relative to central axis normalization dose. Criteria in terms of 1 SD.
[b] Low dose is defined as dose < 7% of normalization dose.
[c] Acceptance criteria, in local dose, depending on detector: ionization chamber (IC) or thermoluminescent dosimeter (TLD). The criteria refer to a confidence interval of 95%.

Table 3. Acceptance criteria (in local dose unless stated otherwise) for dose calculation algorithms for photon beams according to Venselaar *et al* (2001).

Regions	Simple [A] geometry	Complex[B] geometry	More complex[C] geometry
Central beam axis (high dose / low dose gradient)	2%	3%	4%
Build-up / Penumbra region (high dose / high dose gradient)	2 mm or 10%	3 mm or 15%	3 mm or 15%
Outside central beam axis (high dose / low dose gradient)	3%	3%	4%
Outside beam edges (low dose / low dose gradient)	3%[a] (30%)	4%[a] (40%)	5%[a] (50%)
Field width (defined at the 50% level)	2 mm or 1%	2 mm or 1%	2 mm or 1%
Beam fringe[b]	2 mm	3 mm	3 mm

[A] Simple geometry: Homogeneous water phantoms, symmetric fields without accessories.
[B] Complex geometry: Inhomogeneities, missing tissue and irregular, wedged or asymmetric fields.
[C] More complex geometry: Various combinations of the conditions given in B.
[a] Percentages defined relative to the dose on the central axis at the same depth or in the open part of the field in the case of blocked fields. Percentages relative to the local dose are given in brackets.
[b] Distance between the 50% and 90% points in the penumbra

2.4 Assessment of deviations between data sets

The assessment of deviations between calculated (evaluation) and reference data can be a challenging task to perform when large data sets are considered. The terms calculated data and evaluated data will be used synonymously in the text.

The interpretation of the results is facilitated if data are expressed in terms of absolute dose per monitor unit (MU). If normalized data are preferred, the so-called output-factor-normalized dose,

$$d_{OFN}(i) = \frac{D(i)}{D(ref.cond.)}, \tag{1}$$

preserves the absolute dose characteristics of the data. $D(i)$ is the dose per MU at point i, and $D(ref.cond.)$ is the dose per MU under reference conditions (e.g. at 10 cm depth in a 10×10 cm^2 field for photon beams).

Absolute dose per monitor unit data and output-factor-normalized data both enable simultaneous evaluation of the relative dose distribution and the absolute dose level. This concept was used in the present work (Papers I, III

and IV) and is also recommended in ESTRO[4] booklet no. 7 (ESTRO 2004). In Paper II, where the same field size is used throughout the study, a standard normalization relative to the dose at 5 cm depth was used. In the qualitative comparison in the mediastinum case in Paper I normalization relative to the depth of dose maximum was used.

Deviations between calculated and reference data can be expressed in absolute or relative terms regarding dose or, in the presence of high dose gradients, as a geometrical displacement of isodose lines. The relative measure can be expressed as,

(i) the percentage of the local reference data

$$\frac{D_{eval}(i) - D_{ref}(i)}{D_{ref}(i)} \times 100 \quad [\%] \tag{2}$$

(ii) the percentage of the dose at a specific, well-defined point within the reference data

$$\frac{D_{eval}(i) - D_{ref}(i)}{D_{ref}(in\ field)} \times 100 \quad [\%] \tag{3}$$

$D_{eval}(i)$ is the calculated dose per MU at point i and $D_{ref}(i)$ is the reference dose per MU at point i. $D_{ref}(in\ field)$ is the reference dose per MU at a point located at, e.g., the depth of point i ($z(i)$) or the depth of maximum dose (z_{max}), either on the central axis or in an unblocked part of the field. D_{eval} and D_{ref} in Equations 2 and 3 can be replaced by d_{OFN} (Equation 1).

Some of the acceptance criteria for dose calculation algorithms in Tables 2 and 3 are combinations of dose deviations in low dose gradient regions and dta in high dose gradient regions. One way to assess this duality is to calculate both quantities and then either select the smaller value of the two, or let pre-defined regions determine which criterion, dose or distance, should be used (Blomquist *et al* 1996, van't Veld 1997, Venselaar *et al* 2001). Blomquist *et al* (1996) also incorporated the volume concept of ICRU 50 (ICRU 1993), concerning maximum target doses, to facilitate drawing conclusions of the clinical usefulness of the dose distributions.

Cheng *et al* (1996) and Harms *et al* (1998) developed a tool for the evaluation of the composite criterion, where only regions that failed both the dose and the geometrical criteria were identified. The result is a binary function, giving the result pass or fail, where the degree of failure is unknown. A further development of this composite criterion is the γ-concept introduced by Low *et al* (1998). Briefly, the γ-concept combines the spatial distance (Δr) between evaluated and reference points and the corresponding dose differences (ΔD) using acceptance ellipses in dose-distance space. The γ-concept is visualized in Fig. 1. Δr is, depending on the dimension of the evaluation distribution, the
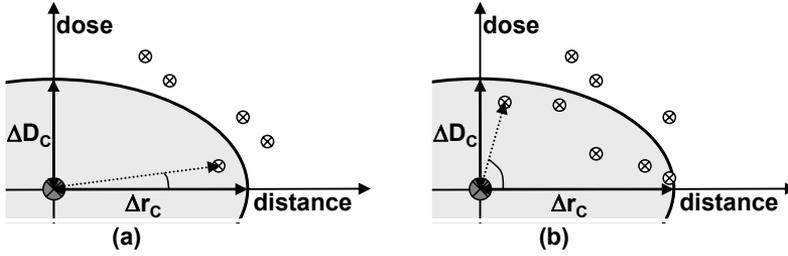
---

[4] European Society for Therapeutic Radiology and Oncology

Figure 1. Schematic illustration of the γ-concept. The reference point (⊗) is located at the origin of the ellipse. Evaluation points (⊗) within the shaded are have Γ<1.0. a) and b) illustrate situations where the distance and the dose criteria dominate, respectively.

resultant distance in the 1D, 2D or 3D Cartesian space. The ellipses are centred on each reference point and the axes of the ellipses are defined by the acceptance criteria: dose difference (ΔD_C) and distance-to-agreement (Δr_C) (see Equations 4 and 5).

$$\Gamma = \sqrt{\frac{\Delta r^2}{\Delta r_C{}^2} + \frac{\Delta D^2}{\Delta D_C{}^2}} \qquad (4)$$

$$\gamma = \min\left(\Gamma\right) \forall \text{ evaluation points} \qquad (5)$$

If preferred, ΔD can be normalized to either local or global dose. The γ-value is defined as the minimum distance in dose-distance space and since the acceptance criteria define the axes of the ellipses, a γ≤1.0 represents fulfilment of the criteria. For points that do not fulfil the criteria, the γ-value provides a measure of the level of disagreement. The angle between the distance axis and the vector defining γ, indicates the relative contribution of Δr and ΔD to γ. The angles 0° and 90° represent pure Δr and ΔD deviations, respectively.

The γ-tool is not symmetric with respect to the evaluated and reference distributions, and the spatial resolution of the evaluation distribution must be small compared with the dta acceptance criteria to provide an accurate γ calculation. The resolution of the evaluation distribution should, as a rule, be 1/3 of the dta criterion (Low and Dempsey 2003). Spatial interpolation of the evaluation data may therefore be necessary. In the above, and in most applications of the γ-concept, an ellipse is used to determine the acceptance region, but other shapes, such as cylinders and cones, can be used (Low *et al* 1998). To overcome the problem of overestimation of the γ-value due to the discrete nature of the evaluation distribution, Depuydt *et al* (2002) used the γ-value as a pass/fail criterion. For the same reason, and to save time, Bakai *et al* (2003) introduced a different formalism to quantify a parameter similar to the γ-value based on the locally observed dose difference between a pair of dose points in conjunction with the dose difference and dta criteria. The elliptical γ-

concept, according to Low *et al* (1998), was used in one and three dimensions in the studies described in Papers III and IV, respectively[5].

The methods described above can lead to a large amount of data. Some of the evaluation points may exceed the acceptance level, but the overall accuracy may still be quite satisfactory. To address this problem the confidence limit, Δ, was introduced, $\Delta=|average\ deviation|+1.5\ SD$ (Welleweerd and van der Zee 1998, Venselaar *et al* 2001, Venselaar and Welleweerd 2001). A sufficient number of data points must be used to obtain statistically reliable results, and it may therefore be necessary to combine data with similar characteristics, e.g., the penumbra region for different field sizes. The confidence limit can exceed the tolerance in either of two ways: (1) the mean deviation of all points is too large, or (2) some points show large deviations translating into too large a SD. The multiplication factor of 1.5 was chosen somewhat arbitrarily but has proven to be valid in clinical practice. For the confidence limit concept with a multiplication factor of 1.5, an acceptable outcome of a test implies that 6.5% of the individual data points exceed the tolerance (1.5 SD is equivalent to a one-sided confidence probability of 0.065 assuming a Gaussian distribution).

Another way to condense data is to generate histograms which give a measure of the level of agreement. This has been performed for the γ-concept where either frequency or cumulative γ-area histograms and γ-volume histograms are used to represent γ information in two and three dimensions, respectively (Spezi 2003, Stock *et al* 2005).

2.5   Conventional measurements

Uncertainties and limitations in conventional measurements are associated with the detector system and the experimental setup used, as well as the stability of the accelerator. Regarding the detector system, the properties of both the detectors and the readout equipment affect the result.

A radiation detector is a device that provides a measurable response when exposed to ionizing radiation. The quantity of interest when a radiation detector is introduced into a medium is often the dose to the medium in the absence of the detector. However, the quantity of interest when measuring beam reference data is in most cases the dose to water, since dose calculation algorithms often calculate the dose to water.

Detectors used in radiotherapy (Kron 1999) can be divided into "point" detectors and multi-dimensional detectors. Commonly used point detectors are silicon diodes, ionization chambers, and TLDs that can be used to assess data at points and in one, two or three dimensions when mounted in an array or when used in scanning mode. Film is a widely used detector for 2D applications, where multiple measurements and/or detectors are used to obtain 3D data. A complete 3D detector is the gel dosimeter, which acquires an entire 3D distribution during one measurement (De Deene 2002).

---

[5] A computer code, partially based on the 2D code in the DICOM-RT toolbox (Spezi *et al* 2002), was written in MATLAB (The MathWorks Inc., Natick, MA, USA).

Depending on beam quality, the type of detector and the phantom, various dosimetric issues must be considered. Some of these are:

- the non-constant medium-to-detector stopping power ratios (Kapur and Ma 1999, Doucet *et al* 2003),
- the hyper-sensitivity of radiographic film to low-energy photons (Palm and LoSasso 2005),
- the enhanced sensitivity of silicon diodes to low-energy photons (Rikner 1985), and
- departures from ideal cavity theory, so-called perturbation effects (Nahum 1996, Mobit *et al* 2000, Doucet *et al* 2003).

The detector/phantom combination determines the number of dose points available for comparison and in most cases *invivo* measurements are limited to easily accessible anatomical sites.

Geometrical inaccuracies associated with the alignment of the accelerator with respect to the phantom and the positioning of the detector also contribute to the uncertainty. A detector positioning uncertainty of ±0.5 mm has been reported (Kosunen *et al* 1993, Blomquist *et al* 1996).

Algorithm input data and beam reference data are often not measured at the same time. Due to the extent of the data required these measurements can last several days or weeks. The data sets can therefore be affected by stability in accelerator performance, e.g., energy, output, flatness and symmetry. The requirements on the accelerators are of the same order as those on the dose calculation algorithms (AAPM 1994, IPEM 1999). Thus, other conditions, which can only be partly compensated for, may be present when beam reference data measurements are performed. For example, Fippel *et al* (1997) found inconsistencies for some geometries in the benchmarking data set for electrons from the National Cancer Institute Electron Collaborative Work Group (Shiu *et al* 1992). These could be explained by the fact that some of the measurements were performed with different accelerators on different days.

It is therefore not trivial to compile self-consistent benchmark data sets for verification of dose calculation algorithms in TPSs (AAPM 1998). Studies where MC-calculated data were used to validate the accuracy and consistency of the measured data set have been reported (Boyd *et al* 2001).

3 The virtual accelerator – A Monte Carlo approach

The Monte Carlo technique is a probabilistic method suitable for solving complex problems such as radiation transport in matter. The statistical distributions used in MC simulations are derived from the underlying physical properties of the processes involved.

MC methods are today widely used in different radiation therapy applications (Rogers and Bielajew 1990, Mackie 1990, Andreo 1991, Ma and Jiang 1999, Rogers 2002, Verhaegen and Seuntjens 2003). It should be emphasized that the accuracy of the MC method depends on the underlying theoretical models, as well as the software implementation and parameters chosen by the user.

3.1 The Monte Carlo method

The trajectories of individual particles are simulated in the MC method by using random numbers to sample the physical processes involved. Each initial particle and all its secondary products are usually referred to as a particle history in MC simulations.

When traversing a medium, e.g., a water phantom, photons undergo relatively few interactions since the mean free path (in water) of high energy photons is of the order of decimetres. The distance to the interaction point and the properties of the interaction can therefore be simulated for individual photons based on total and differential cross-section data.

The simulation of electrons is a more complex task due to the large number of collisions they undergo during the slowing-down process. As an electron and its secondary particles slow down in a material, they can undergo hundreds of thousands of elastic and inelastic collisions until they are locally absorbed. An event-by-event simulation, as for photons, is thus extremely time consuming. This led to the development of the condensed history technique (Berger 1963). In this technique a large number of collisions are condensed into a single electron step where the cumulative effect of energy loss and changes in direction and position are sampled from multiple scatter distributions. The condensed history technique is feasible due to the fact that the majority of the interactions result only in minor changes in energy and direction.

The quantities of interest, e.g., deposited energy, absorbed dose or fluence, are given as the average quantity over a large number of simulated histories, typically 10^6 to 10^9. The MC method usually calculates the absorbed dose to the medium, D_m.

3.2 Use of Monte Carlo in the verification process of dose calculation algorithms in TPSs

The introduction of MC techniques offers a new means of verifying dose calculation algorithms in TPSs. Geometric and dosimetric problems associated with conventional measurements, regarding both detectors and the accelerator,

can be avoided. Data can be assessed in three dimensions and evaluation geometries can easily be added when required without compromising the consistency of the data. Another advantage is that beam reference data can be obtained in what is normally considered unmeasurable geometries, such as in anthropomorphic phantoms based on patient CT data (Ma *et al* 1999, Francescon *et al* 2000, Wang *et al* 2001, Spezi 2003, Haedinger *et al* 2005, Paper IV). The possibility of using anthropomorphic phantoms based on patient CT data is an advantage compared with standard anthropomorphic phantoms, since the phantoms can be varied. MC techniques also allow detailed studies of properties that are difficult or even impossible to measure, such as the dose and fluence due to individual particle types and sources (Ahnesjö 1989, Wieslander *et al* 2001, Papers II and III). The MC method is thus an excellent complement to conventional measurements.

MC methods for dose calculation verification can be applied in several ways. One is to tune the parameters of the MC model to reproduce measured data for specific treatment units in the clinic. The input data to the MC simulation include the parameters of the electron beam exiting the accelerating structure and geometrical specifications of treatment-head components. This tuning process is a rather cumbersome method and deviations may still be present due to inaccuracies in the treatment head geometry or the description of the electron beam (Bieda *et al* 2001, Antolak *et al* 2002, Faddegon *et al* 2005, Popescu and Bush 2005). An alternative method is to describe the properties of the radiation beam based on source models with parameters extracted from measured data. The use of MC methods based on specific clinical treatment units for the verification of dose calculations in TPSs has been described by, e.g., Ma *et al* 1999, Ding *et al* 1999, Francescon *et al* 2000, Lewis *et al* 2000, Miften *et al* 2001, Wieslander *et al* 2001, Yorke *et al* 2002, Martens *et al* 2002, Spezi 2003, Cranmer-Sargison *et al* 2004, Krieger and Sauer 2005, Paelinck *et al* 2005 and Haedinger *et al* 2005, among others.

3.3   The virtual linear accelerator

The approach proposed in this study is to implement a treatment unit, a *virtual accelerator*, in the TPS where the algorithm input data (profiles, depth doses, output factors, etc.) as well as the beam reference data, are generated by MC simulations (Fig. 2, left panel). Thus the consistency of the algorithm input data and the beam reference data is preserved. The MC-generated data are processed and implemented as a complete treatment unit in the TPS (Fig. 2, right panel). This approach enables the use of either source models (Papers I and II), or detailed simulations of the treatment head (Papers III and IV). An advantage of the virtual accelerator is that no difficult and time-consuming tuning of the input data is needed to match an existing accelerator. For the verification of dose calculation algorithms and studies of their inherent limitations (Fig. 2, middle panel) an exact match to an existing accelerator is not necessary. However, the virtual accelerator should be based on realistic data.
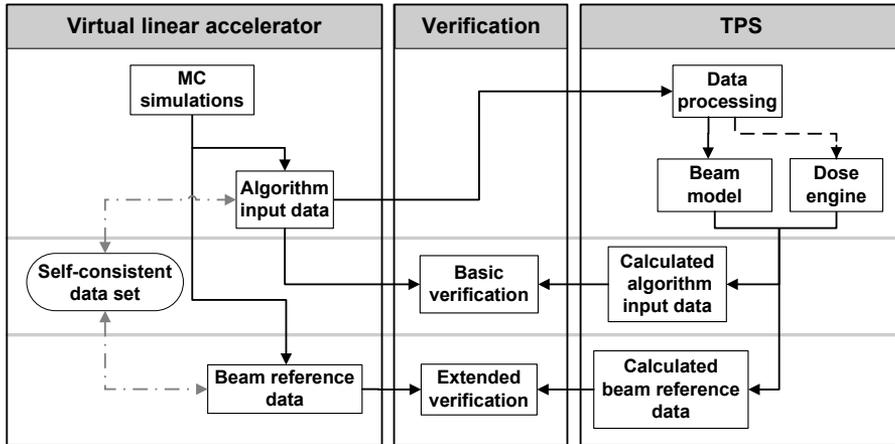
Figure 2. A flow chart visualizing the virtual accelerator concept. The figure shows the fundamental steps in the verification process and their relationships.

3.3.1 The Monte Carlo code

The Monte Carlo simulations in this work were performed with the EGS (Electron-Gamma-Shower) code system for electron and photon transport. Both EGS4 (Nelson *et al* 1985) and its enhanced successor, EGSnrc, (Kawrakow 2000, Kawrakow and Rogers 2001, Kawrakow and Rogers 2002) were used. EGS-based user codes are widely used in different parts of the radiotherapy chain. Examples of EGS code system applications are given below.

- The stopping-power ratios for electron beams used in protocols for absorbed dose determination, e.g., IAEA 2000 and AAPM 1999 (Ding *et al* 1995)
- Perturbation factors for ionization-based dosimetry (Rogers and Treurniet 1999, Mainegra-Hing *et al* 2003, McCaffrey *et al* 2004)
- The design of beam formation systems for optimal beam properties and the resulting dose distributions (Karlsson *et al* 1999, Northey and Zavgorodni 2002, Ye *et al* 2005)
- The calculation of point spread functions used for treatment planning (Mackie *et al* 1988)
- Dose calculation algorithms for treatment planning (Faddegon *et al* 1998, Ma *et al* 1999)
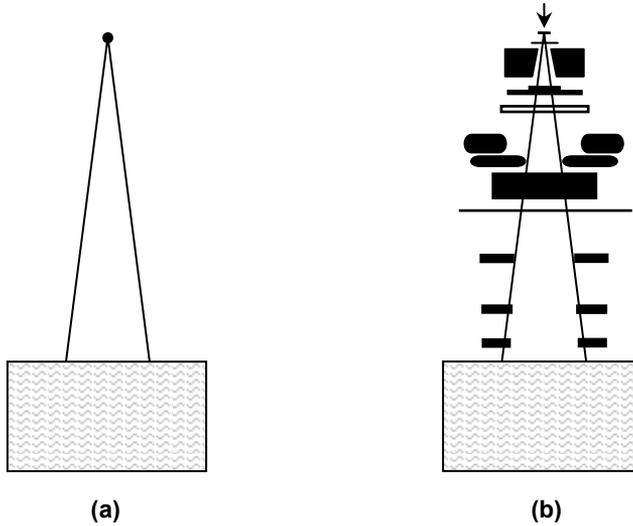- Verification of the consistency in measured data (Boyd *et al* 2001)

Figure 3. Schematics of the photon (a) and electron (b) virtual accelerators.

3.3.2 The virtual photon accelerator

The virtual accelerator for 6 and 18 MV photons, introduced in Paper I, is based on MC simulations with the EGS4 user code XYZP. The simulations were performed in a Cartesian voxel grid. The code was modified to incorporate the possibility of using a photon spectrum as input data for the simulation, as well as the use of divergent beams. The accelerator head was not simulated in detail. The photon beams were instead simulated based on the divergent field possibilities in the MC code in combination with a photon spectrum (see Fig. 3a). To achieve clinical beam qualities a depth-dose equivalent spectrum was used. This simplified accelerator enables a dedicated analysis of the dose calculation in the patient or phantom.

The beam reference data presented in Paper II for the virtual photon accelerator were generated with the EGSnrc user code, DOSXYZnrc (Walters and Rogers 2002). The new version was used due to the improved performance of the code, especially concerning the modelling of interface effects (Kawrakow and Rogers 2001, Verhaegen 2002). The virtual accelerator unit in the TPS based on EGS4-generated data was used since no difference was found between algorithm input data generated by DOSXYZnrc and XYZP.

A modified EGS4 user code was also used to study the dose calculated by the TPS divided into primary[6] and phantom-scatter[7] components (Paper II). If desired, the dose calculated by the modified EGS4 code can be divided into

---

[6] Primary dose: absorbed dose associated with photons interacting with the medium for the first time.

[7] Phantom-scatter dose: absorbed dose associated with photons scattered or created in the phantom/patient.

primary dose and the dose from the first, second and multiple scattering of the photons.

3.3.3 The virtual electron accelerator

Paper III describes a virtual electron accelerator based on detailed simulations of the treatment head for 6, 12 and 18 MeV electrons (see Fig. 3b). The treatment head was modelled with the BEAMnrc code based on generic geometrical specifications of an Elekta Pres*i*ce accelerator (Rogers *et al* 1995, Rogers *et al* 2002). The parameters of the initial electron source in the MC simulations were chosen to produce depth-dose distributions similar to those from common clinical electron beams. The dose distribution in the phantom was simulated with DOSXYZnrc in a Cartesian voxel grid (Walters and Rogers 2002). The user code BEAMnrc is dedicated to the modelling of radiotherapy sources and employs component modules that easily describe the geometry. In addition to information such as charge, energy, position and direction, particles can also be tagged with interaction history. This information can be stored in a so-called phase space file that can be analysed or used as a source input in subsequent simulations with, for example, DOSXYZnrc. The tagging of the particles can be used to group particles based on their interaction history, which enables detailed studies of the beam model used in the TPSs, for example.

3.3.4 Anthropomorphic phantoms

The inhomogeneity corrections in TPSs are commonly based on properties assigned from Hounsfield units (HU) determined from a series of CT images. The virtual accelerator concept enables 3D evaluation of the dose calculation in anthropomorphic phantoms based on patient CT images. Phantoms suitable for the DOSXYZnrc code are constructed by conversion of HU into materials and mass density. In this work, the emphasis was placed on the accuracy of dose calculation algorithms. Therefore, a conversion function from HU to materials and mass density that approximately match that of the TPS was used. The re-sampling of the CT data was also performed in the same way as in the TPS. This minimizes discrepancies due to mis-assignments of media between the virtual accelerator and the TPS. The validity of the specific conversion function used in the TPS was consequently not evaluated.

4 Verification of photon and electron dose calculation algorithms

The usefulness and advantages of the virtual accelerator concept for verification of dose calculation algorithms in TPSs have been demonstrated by studies of the photon algorithms in TMS[8,9] and the electron algorithm in Oncentra MasterPlan (OMP)[8]. The photon algorithms in TMS are the pencil beam (PB) and the collapsed cone (CC) algorithms and the electron algorithm in OMP is MC-based.

This chapter gives a brief overview of the studied dose calculation algorithms for photons and electrons. A review of the algorithms' performance is also given, for the cases of both measurement-based verification and the application of the virtual accelerator. A comprehensive review of photon and electron dose calculations in external beam radiotherapy can be found in e.g., Ahnesjö and Aspradakis (1999), AAPM (2004) and Keall and Hoban (1996).

Dose calculation algorithms used in treatment planning can generally be classified into correction-based or model-based algorithms (Mackie *et al* 1995). In correction-based algorithms the dose distribution in water is first reconstructed from measured data and then corrected to account for the actual treatment conditions, i.e., beam modifier and patient-related properties (surface contour and inhomogeneities). Model-based algorithms derive the dose distribution using physical descriptions of the treatment beam and the energy deposition within the patient. The dose calculation algorithms evaluated in this study are all model-based algorithms.

4.1 Photon dose calculation based on convolution/superposition

The essential components of the convolution/superposition technique are the photon energy fluence and the point spread function (PSF), the latter representing the local transport of released energy. The product of the energy fluence and the mass attenuation coefficient describes the total energy released per unit mass, terma. The point spread function (or energy deposition kernel) describes the energy deposited by secondary particles (charged particles and scattered photons) in volume elements around primary photon interactions as a function of position (see Fig. 4). The convolution of these two entities, the terma and the spatially invariant PSF, yields the dose distribution:

$$D(\vec{r}) = \int_{Vol} T(\vec{r}') \, h(\vec{r} - \vec{r}') dV \; , \tag{6}$$

where T is the terma and h is the PSF (see Fig. 4). The terma is determined by ray-tracing through the patient/phantom taking into account attenuation and the

---

[8] Nucletron B.V.

[9] The PB and the CC algorithms are also implemented in Oncentra MasterPlan.
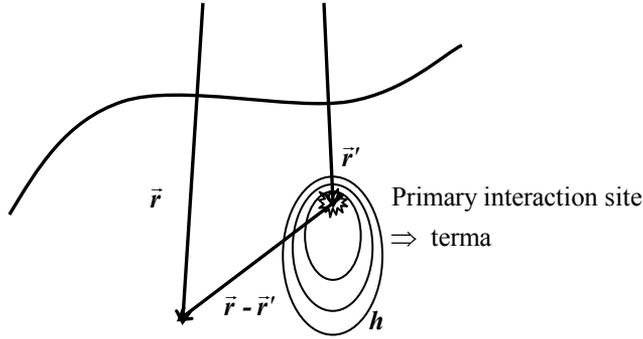
Figure 4. Schematic geometry for the convolution/superposition calculation.

inverse-square law dependence. The PSFs are usually generated for mono-energetic photon beams by Monte Carlo methods (Ahnesjö *et al* 1987, Mackie *et al* 1988). The extension to inhomogeneous geometries is based on modifications of both the terma and the PSF. The use of spatially variant PSFs is also known as superpositioning.

The convolution calculation is, however, very time-consuming. To increase the calculation speed, the collapsed cone approximation was introduced (Ahnesjö 1989). The PSF is divided into a number of cones, each emanating from its origin, where the energy deposited within a cone is collapsed to the central ray of that cone (see Fig. 5). The cones are unevenly distributed, with a larger number of cones in the forward direction due to the forward-peaked energy release from a primary photon interaction. At large distances from the kernel origin, where a cone covers several calculation voxels, the voxel intercepting the cone axis is defined as containing all the deposited energy. The voxels not assigned any energy are compensated by energy from other collapsed cone lines. Therefore, the accuracy of the approximation decreases with increasing distance from the kernel origin. However, the relative importance of this is reduced by the rapid decrease of the PSF with increasing distance from the origin. The dose deposited in a calculation voxel is assigned to the mid-point of the voxel.

Poly-energetic PSFs in water are derived as a weighted sum of mono-energetic PSFs. The PSFs in the CC algorithm in TMS are described by a sum of two exponentials, which can be interpreted as a separation in primary and phantom-scatter components. Beam hardening with depth in the medium and off-axis softening are modelled as part of the terma. The divergence of the beam is accounted for by a slight tilt of the kernels (Ahnesjö 1989). It should be emphasized that the CC algorithm implementation in TMS calculates the absorbed dose to the medium (Ahnesjö 1989, Ahnesjö 2002, Aspradakis *et al* 2003, Paper II).
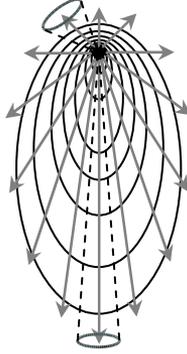
Figure 5. A schematic illustration of cones and the cone lines in the collapsed cone approximation.

Another approach to further increase the calculation speed, is the pre-integration of PSFs in the direction along the beam axis taking the beam attenuation into consideration. This integration yields so-called pencil beam kernels that describe the energy distribution around an infinitely narrow beam (see Fig. 6). The convolution of the impinging energy fluence with the PB kernel yields the dose distribution:

$$D(s,z) = \int \Psi(s',z_0) p(s-s',z) ds' , \tag{7}$$

where $\Psi(z_0)$ is the impinging energy fluence distribution and p the PB kernel expressed as absorbed dose per unit impinging energy fluence (see Fig. 6).

Poly-energetic PB kernels are computed as a linear combination of spectrum-weighted, mono-energetic PB kernels. The use of a spatially invariant energy spectrum ignores effects due to off-axis softening. Pre-integration leads to a semi-infinite slab approximation with overestimation of the calculated dose for small geometries, limited laterally and/or downstream. The PB kernel incorporates energy scattered from points both laterally and downstream of the dose calculation point. If there are no scattering media at these lateral and downstream points the dose will be overestimated.

The PB kernels used in the PB algorithm in TMS are based on the same PSFs as in the CC algorithm and are fitted to a sum of two exponentials describing the lateral energy spread at each depth down to 50.025 cm. The two exponentials can be interpreted as separation into primary and phantom-scatter dose (Ahnesjö *et al* 1992).

In the presence of heterogeneities the equivalent path length (or radiological depth) method for inhomogeneity correction is used for all dose components except for the phantom-scatter dose in the PB algorithm in TMS. This means that the depth-dependent parameters describing the dose components are extracted at a depth in water defined by the radiological depth of the calculation point, i.e., the geometrical depth in water at which the same attenuation would
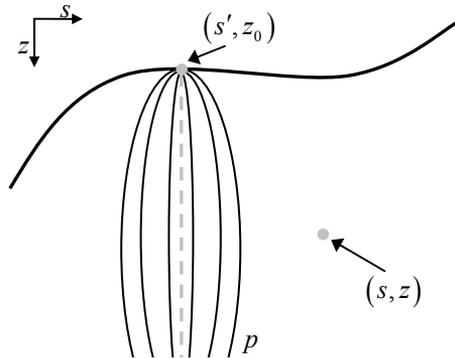
Figure 6. Schematic geometry for the pencil beam calculation.

have been obtained. The phantom-scatter dose is calculated in water and modulated with a correction factor. The PB algorithm in TMS calculates dose to water, D_w.

4.1.1 *Accuracy of the photon dose calculation algorithms*

The PB-calculated dose is insensitive to the phantom thickness distal to the calculation point (Hurkmans *et al* 1995). This missing tissue limitation may be a potential clinical problem when small geometries are involved, such as the tangential field technique for breast treatment and in the head and neck region. Deviations of up to 5-8% have been reported in tangential geometries (Knöös *et al* 1994, Aspradakis *et al* 2003). The relative importance of this semi-infinite slab approximation increases with decreasing energy and increasing field size (Hurkmans *et al* 1995). The reduction in phantom scatter in missing tissue geometries is predicted by the CC algorithm, with reported deviations from measurements within ±2% (Weber and Nilsson 2002, Aspradakis *et al* 2003, Nisbet *et al* 2004).

The PB algorithm does not model the electron transport in media other than water. The magnitude of the disagreement due to this limitation is related to the degree of electron disequilibrium. The increased penumbra width, within a low-density medium, due to the prolonged range of the electrons is not modelled (Knöös *et al* 1995, Aspradakis *et al* 2003, Carrasco *et al* 2004, Krieger and Sauer 2005, Paper I). This lateral transport limitation also gives rise to disagreements in central parts of small fields in low density media (Carrasco *et al* 2004). The CC algorithm models lateral energy transport and therefore more accurately predicts effects due to lateral charged-particle disequilibrium in conjunction with inhomogeneities (Ahnesjö 1989, Weber and Nilsson 2002, Aspradakis *et al* 2003, Carrasco *et al* 2004, Nisbet *et al* 2004, Paelinck *et al* 2005).

Dose reduction laterally of a low density medium due to changes in phantom scatter is not modelled by the PB algorithm, since it assumes water to be the scattering medium. This dose reduction is quite well predicted by the CC algorithm (Aspradakis *et al* 2003).
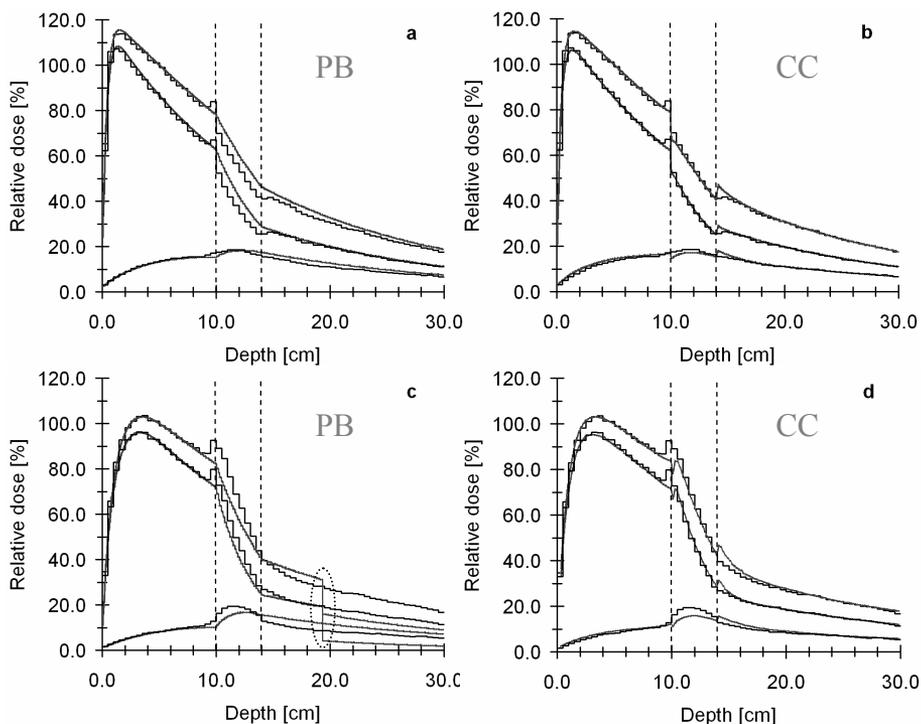
30

Figure 7. Central depth-dose curves for the TiAlV (a, b) and the steel (c, d) phantoms for 6 and 18 MV, respectively (same set-up as in Paper II). Total dose, primary and phantom-scatter dose are shown. Step-shaped curves represent the virtual accelerator results[10] and solid lines the dose calculation algorithms. The discontinuity in primary dose is indicated by the dotted region in c.

Interface effects in the presence of inhomogeneities are not modelled either by the PB algorithm (Carrasco *et al* 2004, Nisbet *et al* 2004). The CC algorithm is generally better at predicting interface effects. Changes in the scatter distribution, relative to water, in the presence of inhomogeneities are, however, not modelled by the CC algorithm, since the PSF is generated in water. This leads to limited accuracy in the prediction of the dose at interfaces (Martens *et al* 2002, Carrasco *et al* 2004, Nisbet *et al* 2004, Paelinck *et al* 2005, Paper II). The virtual accelerator results for common high-Z materials used in hip prostheses show that the CC algorithm overestimates the dose downstream of the high-Z region. The increase in the dose laterally of the high-Z region is only partially modelled and the effects in front of the region due to the increased backscatter are practically not modelled at all. The coarse resolution of the cones in these directions (laterally and backwards) also contributes to the observed differences. This is shown in Fig. 7 and Figs. 1 and 4 in Paper II.

---

[10] Virtual accelerator simulations for the separation of primary and phantom-scatter dose were performed with an EGS4 based code in 5 mm voxels.

Table 4. Deviation (%) in the beam intersection point between the virtual accelerator and the CC and PB algorithms for 18 MV in two hypothetical prostate patients with CoCrMo hip prostheses.

	Algorithm	
	PB	CC
Four-field technique		
Uni-lateral prosthesis	-4	1
Bi-lateral prostheses	-10	2
Three- field technique		
Uni-lateral prosthesis	-7	1
Bi-lateral prostheses	-16	3

The dose in water beyond regions (excluding interface effects) of non-water-equivalent material is rather well predicted by both algorithms. For air, bone, and lung-equivalent media, the reported data are within 1-3% of measurements (Nisbet *et al* 2004, Carrasco *et al* 2004, Paelinck *et al* 2005). The deviations are generally larger for media of higher Z, i.e., media commonly used for hip prostheses (Roberts 2001, Paper II). The dose predicted by the CC algorithm beyond the high-Z regions (excluding interface effects) is in better agreement with the virtual accelerator results than the PB algorithm predictions. The agreement of the CC data is within -2 to 5% and -1 to 7% at 6 cm beyond the high-Z regions for 6 and 18 MV, respectively (see Table 2 in Paper II).

Within clinically relevant geometrical depths, the presence of high-Z media may result in radiological depths that are greater than the depth of the pre-integrated PB kernel. In Paper II, a significant deficiency was reported in the calculation model or its implementation with respect to the calculated dose at radiological depths greater than the depth of the pre-integrated PB kernel. A differentiated study of the primary and the phantom-scatter dose revealed that the deficiency was related to a large discontinuity in the primary dose. This can be seen in Fig. 7 panel c. A physical depth greater than 19 cm corresponds to a radiological depth greater than 50.025 cm.

Table 4 shows the deviation in percent in the beam intersection point between the virtual accelerator and the CC and PB algorithms for two hypothetical prostate cases, one with a uni-lateral CoCrMo prosthesis and one with bi-lateral CoCrMo prostheses. Equal doses at z_{max} and a fixed source-skin-distance (SSD) were used in a three-field technique (one anterior and two lateral fields) and a four-field box technique (one anterior, one posterior and two lateral fields). The above mentioned discontinuity in the primary dose for physical depths greater than 19 cm is the reason for the larger discrepancies for the PB cases.

The ability of the virtual accelerator to separate the primary and phantom-scattered dose can be used to study the influence of inhomogeneities on these components. This possibility was used to evaluate the modelling of inhomogeneities by the PB and CC algorithms (Paper II). This differentiated
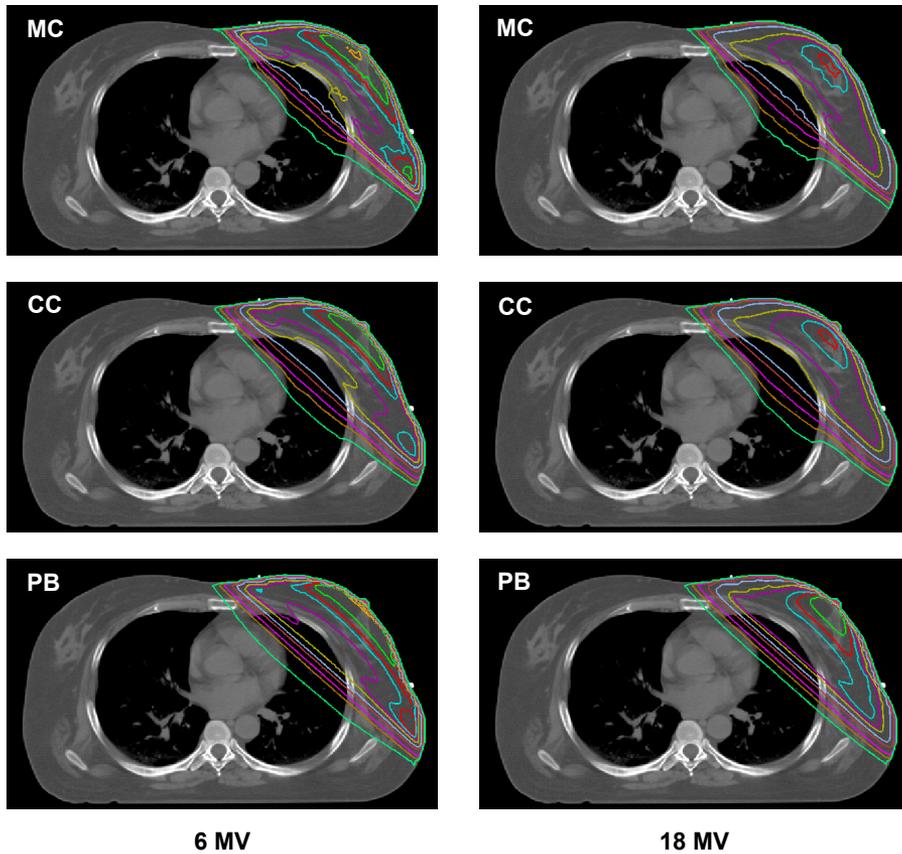
6 MV   **18 MV**

Figure 8. Dose distributions, at the isocenter level, calculated using the virtual accelerator (MC) and the CC and PB algorithms for a tangential treatment of the breast for 6 (left) and 18 MV (right). Isodose levels shown are 5, 10, 20, 50, 70, 90, 95, 100, 102.5, 105 and 110%.

study showed that the greater disagreement beyond the high-Z region (excluding interface effects) of the PB algorithm compared with the CC algorithm was due to discrepancies in the phantom-scattered dose (see Fig. 7). Both the PB and CC algorithms predict the primary dose quite accurately apart from the expected differences within the high-Z region for the PB data, since the PB algorithm calculates D_w.

Another useful application of the virtual accelerator is illustrated in Fig. 8 which shows comparisons between virtual accelerator results (denoted MC in the figure) and the PB and CC algorithms for tangential treatment of a breast. Results for both 6 MV and 18 MV beams are presented. Each plan is output normalized and presented relative to the virtual accelerator plan.

Concluding remarks regarding the photon dose calculation algorithms

The accuracy of the PB algorithm depends on the level of inhomogeneity and missing tissue. The differences between the two algorithms are therefore small in, for example, pelvis cases whereas they are greater in lung and breast cases (Aspradakis *et al* 2003, Irvine *et al* 2004). The CC algorithm is preferable if metal implants are involved (Paper II).

During verification of the dose calculation algorithms in heterogeneous phantoms, the fact that the PB and CC algorithms calculate D_w and D_m, respectively, should be considered. This should also be borne in mind when evaluating treatment plans based on CC calculations. The CC dose calculation is voxel-based which can lead to undesired smoothing effects in both the dose and density distribution if large voxel sizes are used (Weber and Nilsson 2002, Aspradakis *et al* 2003).

Inhomogeneity corrections are based on HU determined by a series of CT images or on manually assigned values. TMS has a built-in fixed calibration curve, where HU are converted to mass densities and a selection of a few standard tissues/materials. The validity of this fixed conversion should be tested by the user (Cozzi *et al* 1998). For example, Roberts (2001) found that both titanium and steel are mapped into the same mass density and material during the creation of the density matrix based on CT data, i.e., that of steel.

4.2 Electron dose calculation based on the Monte Carlo method

The dose calculation algorithm for electrons in OMP is based on a multi-source beam model combined with a MC code, the VMC++ code (Kawrakow and Fippel 2000, Kawrakow 2001), for the in-patient dose calculation. The beam model consists of a parameterized source phase space (SPS), derived from measured data, which describes the electron beam near the secondary scattering foil. This SPS consists of an energy spectrum and five parameters describing the lateral and angular distribution of the electrons. The SPS is propagated through the treatment head, with a dedicated fast MC code combined with pre-calculated scatter kernels, down to just above the last collimating structure, resulting in an exit phase space (EPS) (Ahnesjö *et al* 2000, Traneus *et al* 2001). The parameterized EPS provides the dose calculation engine, the MC code VMC++, with electrons. Detailed benchmarking has shown that the VMC++ code can agree with EGSnrc within the sub-percent level (Kawrakow and Fippel 2000).

The dose from contaminant photons produced in the treatment head is considered separately by an analytical model with parameters extracted from measured data in the bremsstrahlung tail (Nucletron 2005).

The calculated dose can be separated into the dose from *direct electrons* that have not interacted in the applicator, *indirect electrons* that have interacted in the applicator (those modelled by the scatter kernels), and *contaminant photons* from the treatment head. The dose calculation is performed in a voxel grid where the voxel size is automatically set by the TPS and is determined by the size of the patient. The algorithm can calculate either D_w or D_m.

4.2.1 *Accuracy of the electron dose calculation algorithm*

Dose calculations in homogeneous water phantoms have been evaluated for both standard SSD and extended SSD, as well as for oblique incidence. This was performed for applicators with standard inserts (open field) and custom-made inserts (circular and rectangular) using the virtual accelerator based on a Monte Carlo model of an Elekta Prec*i*se accelerator (Paper III). A similar study based on measured data from a Siemens KD-2 accelerator has also been reported (Cygler *et al* 2004).

The differences observed, in depth doses and profiles, by Cygler *et al* (2004) are in the range of 2%[11], with a slightly larger deviation in the build-up region (3%) and for the oblique incidence cases (3.5%). They estimated the overall uncertainty of the measurements to be less than 2.0% and the spatial resolution was 1.0 mm.

The results for the virtual accelerator (Paper III) are mainly in agreement with the findings of Cygler *et al* (2004), except for some discrepancies associated with large applicators for high energies, and patient-specific inserts. For 18 MeV, the dose calculation algorithm underestimates the dose profile laterally by 2-7% (local dose) for the larger applicators (14×14 and 20×20 cm²) (see Fig. 2 in Paper III). This discrepancy is probably the result of the small difference between the diaphragm collimation and the field edge for these energy/applicator combinations. Under these conditions the relative importance of approximations and possible deficiencies in the TPS beam model may be significant. This type of discrepancy has also been observed for some clinical Elekta accelerators.

The discrepancies for the insert with a 10×10 cm² opening in the 14×14 cm² applicator for 6 MeV are also seen laterally in the profiles, where the dose calculation algorithm overestimates the dose by 3% (local dose). The ability of the virtual accelerator to separate direct and applicator-scatter components of the electron dose reveals that this is mainly due to overestimation of dose from direct electrons. The dose from indirect electrons is also overestimated laterally, but the relative contribution to the dose is low.

A comparison of the contaminant photon dose in the bremsstrahlung tail shows that the TPS does not model the contaminant photons generated in the insert or the modulation of the accelerator-generated photons by the insert (see Fig. 9 and Fig. 7 in Paper III). A model deficiency associated with a large underestimation of the dose from contaminant photons generated in the treatment head was found in the first implementation of the virtual accelerator, see Fig. 9. The deficiency was resolved by the vendor and the algorithm input data were processed a second time.

The accuracy of the calculated dose distribution in the presence of inhomogeneities has been studied for schematic geometries and in clinical cases (Paper IV). Cygler *et al* (2004) have also reported results for both high- and low-density inhomogeneities in schematic geometries of increasing complexity.

---

[11] Dose differences in percentage of the dose at z_{max} in a homogeneous water phantom.
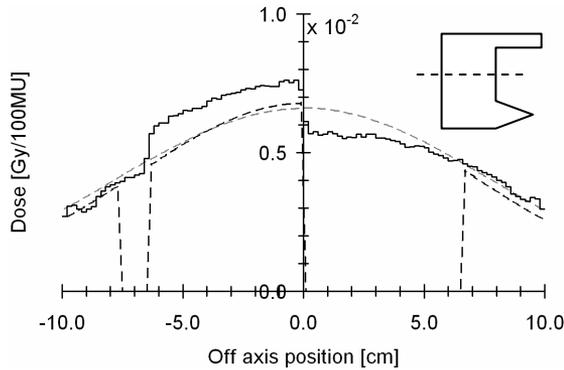
Figure 9. Contaminant photon dose profiles in the bremsstrahlung tail at 5 cm depth for the 6 MeV house-shaped insert in the 14×14 cm^2 applicator. The step-shaped curve represents virtual accelerator results, and the black and grey dashed curves represent the first and second implementation of data into the TPS, respectively.

Their results show larger differences for the inhomogeneous geometries than in homogeneous water phantom cases, as expected. For the simplest geometry, the aluminium slab, the measurements and calculations were within 3% (z_{max} dose). For the bone and air cylinder cases, discrepancies of 5-10% were observed in the vicinity of the heterogeneity, where the higher values in this range correspond to the air case. For the case with the largest degree of complexity, the trachea and spine phantom, the largest discrepancies found were 8%. They concluded that the observed differences could be partly attributed to a too large voxel size, which was 3.0 to 4.0 mm in their study.

The ability of the virtual accelerator to assess data in three dimensions was used to evaluate the performance of the electron algorithm in anthropomorphic phantoms for four cases of electron treatment: nose, parotid gland, thorax wall and spinal cord (Paper IV). Three schematic bone and air geometries were also studied. The data were evaluated in three dimensions using the γ-concept (Equations 4 and 5).

The agreement for the phantoms containing air and bone is better than that reported by Cygler *et al* (2004). For the 0.02 Gy/2 mm (per Gy in z_{max}) criteria, only about 2% of the volume receiving a dose above 0.85 Gy per 100 MU for 18 MeV have γ-values larger than unity (see Table 2 in Paper IV). This better agreement than that obtained by Cygler *et al* (2004) is probably due to the smaller voxel size used (2 mm) and the fact that the same voxel size was used in both set-ups. A study of the contaminant photon dose component in the dose calculation algorithm revealed that the dose was calculated as D_w, regardless of the calculation mode (D_w or D_m) used (see Fig. 2 in Paper IV).

For the clinical cases studied (Paper IV), i.e., thorax wall, parotid gland, nose and spinal cord, it can be concluded that the agreement between the virtual accelerator results and the dose calculation algorithm is generally good. With the 0.03 Gy/3 mm (per Gy in z_{max}) criteria, even for the worst cases, only a small volume of about 5.5-7.5 cm^3 has γ-values greater than unity (see Table 3

in Paper IV). This is well within the acceptance criteria stipulated by Van Dyk *et al* (1993), Table 2. Adopting the optimal goal criteria of 0.02 Gy/2 mm, 92% of the volume receiving more than 0.85 Gy/100 MU has γ-values less than unity for the worst case. The corresponding value for the volume receiving more than 0.10 Gy/100 MU is 98%.

Concluding remarks regarding the electron dose calculation algorithm

Since the algorithm is based on a Monte Carlo technique, the dose distributions are subject to statistical noise. The number of histories needed to achieve a clinically acceptable statistical uncertainty has been proposed to be 50 000 histories per cm² (cubic voxels with 3.0 to 5.0 mm sides were used). This gives a statistical uncertainty of about 1.5% or less (Cygler *et al* 2004, Cygler *et al* 2005). In the studies described in Papers III and IV, one million histories per cm² were used. This relatively large number of histories was chosen to minimize the influence of the statistical noise during the evaluation of the dose calculation.

In the studies by Cygler *et al* (2004) and Ding *et al* (2005) some of the observed discrepancies were attributed to the relatively large voxel size used in the dose calculations. This leads to a large smoothing effect of doses, especially in high-dose gradients, as well as of the material and density distribution. Effects due to the positioning of the voxel grid were also seen. Mora *et al* (2001) stated that a voxel size of 3 mm or less should be used in MC-based dose calculations for treatment planning. It is therefore of great importance that this parameter can be controlled by the user. It should also be easy to assess visually in the TPS to facilitate the interpretation of effects traceable to the voxelisation of the patient or phantom.

The MC-based algorithm is, as expected, superior to the PB-based algorithms in the presence of inhomogeneities (Ding *et al* 2005, Paper IV). However, further improvements regarding, for example, the contaminant photon dose and the electron beam model, are necessary (Papers III and IV).

5   Conclusions

The virtual accelerator concept, where both algorithm input data and beam reference data are generated with MC methods, has been found to be an advantageous approach to the verification of dose calculation algorithms for both photons and electrons. For verification of dose calculation algorithms and studies of their inherent limitations, an exact match to an existing accelerator is not necessary. The difficult and time-consuming tuning procedure, where the MC input data are iteratively modified to match an existing accelerator, can therefore be avoided.

A virtual electron accelerator incorporating a complete model of the treatment head for 6, 12 and 18 MeV electrons was generated. The implementation of this electron accelerator was generally successful for all energies, exceptions being for the larger applicators for 18 MeV, with notable deviations laterally in the profile data. These deviations are associated with shortcomings in the beam model of the TPS and have also been seen for some clinical accelerators from the same vendor. A virtual accelerator, based on a simplified treatment head, was also successfully implemented for 6 and 18 MV photons.

The virtual photon accelerator was used to demonstrate the limitation of the PB algorithm in a mediastinum geometry. The ability of the virtual photon accelerator to generate both total dose and the primary and phantom-scattered components was used to study the performance of the PB and the CC algorithms in the presence of metallic implants.

The virtual electron accelerator was used to study the performance of the MC-based dose calculation algorithm in homogeneous and inhomogeneous phantoms. Studies of the beam model and the handling of patient-specific inserts in the electron algorithm were possible due to the capability of the virtual accelerator to separate the total dose into the direct and applicator-scatter components of the electron dose and the photon contaminant dose.

The possibility of differentiated studies of beam models and the subsequent dose calculations in TPSs are advantages of the virtual accelerator. Other advantages of the virtual accelerator are the possibility of generating 3D beam reference data and constructing anthropomorphic phantoms based on patient CT data. This feature has been used to compare *a)* the performance of the PB and CC algorithms with the virtual accelerator in the case of tangential breast treatment, and *b)* the performance of the electron algorithm in three dimensions for four cases of electron treatment: nose, parotid gland, thorax wall and spinal cord.

The virtual accelerator concept offers a new means of verifying dose calculation algorithms in treatment planning systems. Properties that are difficult or even impossible to assess based on conventional measurements, e.g., dose and fluence from individual particle types and sources, can be studied. Problems associated with conventional measurements, e.g., detector limitations and accelerator stability can be avoided. The flexibility of the virtual accelerator

is high since additional beam reference data can be acquired without compromising the consistency. Beam reference data can be obtained in three dimensions in anthropomorphic phantoms, based on patient CT data, for specific treatment sites and techniques. This enables evaluation of the dose distributions and the consequences of the inherent limitations of the dose calculation algorithm in clinical situations. The virtual accelerator increases the users' understanding of the possibilities and limitations of the dose calculation algorithm.

The possibility of comprehensive differentiated studies of the beam model and the subsequent dose calculation is also valuable for vendors. Further improvements in the overall performance of the dose calculation algorithms are facilitated as well as the isolation and identification of implementation deficiencies. The virtual accelerator concept is therefore an excellent complement to conventional measurements and analytical models.

6 Future development

Of the dose calculation algorithms currently available, MC is generally considered to be the most accurate (Mohan 1997). Commercial MC-based algorithms for electron beam treatment planning are being made available by several vendors and are being planned for photon beams. However, there is still a need for investigations of the accuracy achievable and the limitations of dose calculation algorithms. The MC-based algorithms that calculate the dose in the patient by sourcing data from a beam model may employ various approximations to achieve reasonable calculation speed in a clinical situation. The ability of the beam models to accurately account for the characteristics of the beam exiting the treatment head also determines the level of accuracy achievable.

The virtual photon accelerator presented in Papers I and II was used to verify the dose calculation in the patient/phantom. To enable comprehensive investigations of the beam models used in TPSs, this simplified accelerator should be complemented with a virtual accelerator based on detailed MC simulations of the treatment head.

Virtual accelerators should be implemented in a number of TPSs to facilitate extensive cross-comparison of the performance of different dose calculation algorithms. Virtual accelerators based on treatment heads with different designs may also be needed since the performance of the beam models of the TPSs may depend on the beam formation system used (Paper III).

Comprehensive benchmarking data sets based on the virtual accelerator concept should be made available for verification of dose calculation algorithms in TPSs for both photons and electrons. Conventional benchmarking data sets based on measurements are limited to data at specific points, are static, and may have consistency problems (Shiu *et al* 1992, AAPM 1995, Gifford *et al* 2002, Venselaar and Welleweerd 2001). It is difficult or even impossible to add new verification geometries while maintaining consistency, since the treatment units previously used for the collection of data may be outdated or may have been replaced.

A benchmarking data set based on the virtual accelerator concept can comprise the whole 3D dose distribution for all geometries. Consequently, the individual user can decide if a full 3D evaluation should be performed or if a subset of 1D or 2D distributions should be used. The flexibility of the data set will be high since new geometries for verification and algorithm input data can easily be added without compromising the consistency. Data intended for the analysis of beam models and in-patient dose calculations should be available for TPSs from different vendors. The data should be accessible in a well-known digital format for easy access and use in TPSs and other software.

A benchmarking data set based on the virtual accelerator concept would be an excellent tool for both users and vendors. It would be of great value in the verification of dose calculation algorithms due to its flexibility and the possibility of performing studies of beam models and subsequent dose calculations.

Acknowledgements

Many people have contributed to the completion of this thesis. I wish to express my deepest gratitude to:

Tommy Knöös for all his support and for introducing me to the field of Monte Carlo simulations and treatment planning. Thanks for endless hours of computer coding and maintenance.

Michael Ljungberg for all his help.

Per Nilsson, for his encouragement and support.

All my friends and colleagues at Radiation Physics at Lund University hospital for their help, fruitful discussions and for providing a wonderful atmosphere both during and after work hours.

Anders Ahnesjö, *Lars Weber* and *Erik Traneus* for their assistance with the treatment planning systems. Special thanks to Lars and Erik for implementing the virtual accelerators in the systems.

Daryoush Sheikh-Bagheri for the coding of DOSXYZ for dose component separation and *Maria Aspradakis* for the initial ideas on how to perform the modifications to the XYZP code.

Elekta for supplying the accelerator information.

Helen Sheppard and *Anne Findlater-Jonasson* for proof-reading of manuscripts.

My friends and family for their help, encouragement and fun moments during the years.

Most of all, I would like to thank *Dan*, for his patience, never-ending support and for putting up with my ups and downs.

References

AAPM 1991 American Association of Physicists in Medicine, Clinical electron-beam dosimetry, Report of the American Association of Physicists in Medicine Radiation Therapy Committee Task Group No. 25 *Med. Phys.* **18** 73-109

AAPM 1994 American Association of Physicists in Medicine, Comprehensive QA for radiation oncology, Report of the American Association of Physicists in Medicine Radiation Therapy Committee Task Group No. 40 *Med. Phys.* **21** 581-618

AAPM 1995 American Association of Physicists in Medicine, Radiation treatment planning dosimetry verification, A test package prepared by the American Association of Physicists in Medicine Radiation Therapy Committee Task Group No. 23 (Woodbury NY: American Institute of Physics)

AAPM 1998 American Association of Physicists in Medicine, Quality assurance for clinical radiotherapy treatment planning, Report of the American Association of Physicists in Medicine Radiation Therapy Committee Task Group No. 53 *Med. Phys.* **25** 1773-1829

AAPM 1999 American Association of Physicists in Medicine, Protocol for clinical reference dosimetry of high-energy photon and electron beams, Report of the American Association of Physicists in Medicine Radiation Therapy Committee Task Group No. 51 *Med. Phys.* **26** 1847-1870

AAPM 2004 American Association of Physicists in Medicine, Tissue inhomogeneity corrections for megavoltage photon beams, Report of the American Association of Physicists in Medicine Radiation Therapy Committee Task Group No. 65 (Madison WI: Medial Physics Publishing)

Ahnesjö A, Andreo P and Brahme A 1987 Calculation and application of point spread functions for treatment planning with high energy photon beams *Acta Oncol.* **26** 49-56

Ahnesjö A 1989 Collapsed cone convolution of radiant energy for photon dose calculation in heterogeneous media *Med. Phys.* **16** 577-592

Ahnesjö A 1991 Dose calculation methods in photon beam therapy using energy deposition kernels PhD Thesis Stockholm University

Ahnesjö A, Saxner M and Trepp A 1992 A pencil beam model for photon dose calculation *Med. Phys.* **19** 263-273

Ahnesjö A and Aspradakis M M 1999 Dose calculations for external photon beams in radiotherapy *Phys. Med. Biol.* **44** R99-R155

Ahnesjö A, Traneus E and Åsell M 2000 Generation of phase space data for electron beam Monte Carlo treatment planning *Radiother. Oncol.* **56** (Suppl.1) S79

Ahnesjö A 2002, personal communication

Andreo P 1991 Monte Carlo techniques in medical radiation physics *Phys. Med. Biol.* **36** 861-920

Antolak J A, Bieda M R and Hogstrom K R 2002 Using Monte Carlo methods to commission electron beams: A feasibility study *Med. Phys.* **29** 771-786

Aspradakis M M, Morrison R H, Richmond N D and Steele A 2003 Experimental verification of convolution/superposition photon dose calculations for radiotherapy treatment planning *Phys. Med. Biol.* **48** 2873-2893

Bakai A, Alber M and Nüsslin F 2003 A revision of the γ-evaluation concept for the comparison of dose distributions *Phys. Med. Biol.* **48** 3543-3553

Berger M 1963 Monte Carlo calculation of the penetration and diffusion of fast charged particles In: Methods in computational physics vol. I Alder B, Fernbach S and Rotenberg M Eds. (New York, NY: Academic press)

Bieda M R, Antolak J A and Hogstrom K R 2001 The effect of scattering foil parameters on electron-beam Monte Carlo calculations *Med. Phys.* **28** 2527-2534

Blomquist M, Karlsson M and Karlsson M 1996 Test procedures for verification of an electron pencil beam algorithm implemented for treatment planning *Radiother. Oncol.* **39** 271-86

Boyd R A, Hogstrom K R, Antolak J A and Shiu A S 2001 A measured data set for evaluating electron-beam dose algorithms *Med. Phys.* **28** 950-958

Brahme A, Chavaudra J, Landberg T, McCullough E C, Nüsslin F, Rawlinson J A, Svensson G and Svensson H 1988 Accuracy requirements and quality assurance of external beam therapy with photons and electrons *Acta Oncol.* Suppl. 1

Carrasco P, Jornet N, Duch M A, Weber L, Ginjaume M, Eudaldo T, Jurado D, Ruiz A and Ribas M 2004 Comparison of dose calculation algorithms in phantoms with lung equivalent heterogeneities under conditions of lateral electronic disequilibrium *Med. Phys.* **31** 2899-2911

Cheng A, Harms W B, Gerber R L, Wong J W and Purdy J A 1996 Systematic verification of a three-dimensional electron beam dose calculation algorithm *Med. Phys.* **23** 685-693

Cozzi L, Fogliata A, Buffa F and Bieri S 1998 Dosimetric impact of computed tomography calibration on a commercial treatment planning system for external radiation therapy *Radiother. Oncol.* **48** 335-338

Cranmer-Sargison G, Beckham W A and Popescu I A 2004 Modelling an extreme water-lung interface using a single pencil beam algorithm and the Monte Carlo method *Phys. Med. Biol.* **49** 1557-1567

Cygler J E, Daskalov G M, Chan G H and Ding G X 2004 Evaluation of the first commercial Monte Carlo dose calculation engine for electron beam treatment planning *Med. Phys.* **31** 142-153

Cygler J E, Lochrin C, Daskalov G M, Howard M, Zohr R, Esche B, Eapen L, Grimard L and Caudrelier J M 2005 Clinical use of a commercial Monte Carlo treatment planning system for electron beams *Phys. Med. Biol.* **50** 1029-1034

Dahlin H, Lamm I-L, Landberg T Levernes S and Ulsø N 1983 User requirements on CT-based computed dose planning systems in radiation therapy *Acta Radiol. Oncol.* **22** 397-415

De Deene Y 2002 Gel dosimetry for the dose verification of intensity modulated radiotherapy treatments *Z. Med. Phys.* **12** 77-88

Delaney G, Jacob S, Featherstone C and Barton M 2005 The role of radiotherapy in cancer treatment: estimating optimal utilization from a review of evidence-based clinical guidelines *Cancer* **104** 1129-1137

Depuydt T, Van Esch A and Huyskens D P 2002 A quantitative evaluation of IMRT dose distributions: refinement and clinical assessment of the gamma evaluation *Radiother. Oncol.* **62** 309-319

Ding G X, Rogers D W O and Mackie T R 1995 Calculation of stopping-power ratios using realistic clinical electron beams *Med. Phys.* **22** 489-501

Ding G X, Cygler J E, Zhang G G and Yu M K 1999 Evaluation of a commercial three-dimensional electron beam treatment planning system *Med. Phys.* **26** 2571-2580

Ding G X, Cygler J E, Yu C W, Kalach N I and Daskalov G 2005 A comparison of electron beam dose calculation accuracy between treatment planning systems using either a pencil beam or a Monte Carlo algorithm *Int. J. Radiat. Oncol. Biol. Phys.* **63** 622-633

Doucet R, Olivares M, DeBlois F, Podgorsak E B, Kawrakow I and Seuntjens J 2003 Comparison of measured and Monte Carlo calculated dose distributions in inhomogeneous phantoms in clinical electron beams *Phys. Med. Biol.* **48** 2339-2354

Dutreix A 1984 When and how can we improve precision in radiotherapy? *Radiother. Oncol.* **2** 275-292

ESTRO 2004 European Society for Therapeutic Radiology and Oncology, Quality assurance of treatment planning systems practical examples for non-IMRT photon beams *booklet no. 7* (Brussels: ESTRO)

Faddegon B, Balogh J, Mackenzie R and Scora D 1998 Clinical considerations of Monte Carlo for electron radiotherapy treatment planning *Radiation Physics Chemistry* **53** 217-27

Faddegon B, Schreiber E and Ding X 2005 Monte Carlo simulation of large electron fields *Phys. Med. Biol.* **50** 741-753

Fippel M, Kawrakow I and Friedrich K 1997 Electron beam dose calculations with the VMC algorithm and the verification data of the NCI working group *Phys. Med. Biol.* **42** 501-520

Francescon P, Cavedon C, Reccanello S and Cora S 2000 Photon dose calculation of a three-dimensional treatment planning system compared to the Monte Carlo code BEAM *Med. Phys.* **27** 1579-1587

Gifford K A, Followill D S, Liu H H and Starkschall G 2002 Verification of the accuracy of a photon dose-calculation algorithm *J. Appl. Clin. Med. Phys.* **3** 26-45

Giraud P, Elles S, Helfre S, De Rycke Y, Servois V, Carette M-F, Alzieu C, Bondiau P-Y, Dubray B, Touboul E, Housset M, Rosenwald J-C and Cosset J-M 2002 Conformal radiotherapy for lung cancer: different delineation of the gross tumour volume (GTV) by radiologists and radiation oncologists *Radiother. Oncol.* **62** 27-36

Haedinger U, Krieger T, Flentje M and Wulf J 2005 Influence of calculation model on dose distribution in stereotactic radiotherapy for pulmonary targets *Int. J. Radiat. Oncol. Biol. Phys.* **61** 239-249

Harms W B, Low D A, Wong J W and Purdy J A 1998 A software tool for the quantitative evaluation of 3D dose calculation algorithms *Med. Phys.* **25** 1830-1836

Herman M G 2005 Clinical use of electronic portal imaging *Semin. Radiat. Oncol.* **15** 157-167

Hurkmans C, Knöös T, Nilsson P, Svahn-Tapper G and Danielsson H 1995 Limitations of a pencil beam approach to photon dose calculations in the head and neck region *Radiother. Oncol.* **37** 74-80

IAEA 2000 International Atomic Energy Agency, Absorbed dose determination in external beam radiotherapy: An international code of practice for dosimetry based on standards of absorbed dose to water *Technical reports series no. 398* (Vienna: IAEA)

IAEA 2004 International Atomic Energy Agency, Commissioning and quality assurance of computerized planning systems for radiation treatment of cancer *Technical reports series no. 430* (Vienna: IAEA)

ICRU 1976 International Commission on Radiation Units and Measurements, Determination of absorbed dose in a patient irradiated by beams of X or gamma rays in radiotherapy procedures *ICRU Report 24* (Washington, DC: ICRU)

ICRU 1987 International Commission on Radiation Units and Measurements, Use of computers in external beam radiotherapy procedures with high-energy photons and electrons *ICRU Report 42* (Bethesda, MD: ICRU)

ICRU 1993 International Commission on Radiation Units and Measurements, Prescribing, recording, and reporting photon beam therapy *ICRU Report 50* (Bethesda, MD: ICRU)

IPEM 1999 Institution of Physics and Engineering in Medicine, Physics Aspects of Quality Control in Radiotherapy, Report no. 81 (Yorke: IPEM)

IPEM 2003 Institution of Physics and Engineering in Medicine, The IPEM code of practice for electron dosimetry for radiotherapy beams of initial energy from 4 to 25 MeV based on an absorbed dose to water calibration *Phys. Med. Biol.* **48** 2929-2970

IPEMB 1996 Institution of Physics and Engineering in Medicine and Biology, A guide to commissioning and quality control of treatment planning systems, Report no. 68 (Yorke: IPEM)

Irvine C, Morgan A, Crellin A, Nisbet A and Beange I 2004 The clinical implications of the collapsed cone planning algorithm *Clin. Oncol.* **16** 148-154

Jaffray D A 2005 Emergent technologies for 3-dimensional image-guided radiation delivery *Semin. Radiat. Oncol.* **15** 208-216

Johansson K-A 1982 Studies of different methods of absorbed dose determination and a dosimetric intercomparison at the Nordic radiotherapy centres PhD Thesis University of Gothenburg

Kapur A and Ma C-M 1999 Stopping-power ratios for clinical electron beams from a scatter-foil linear accelerator *Phys. Med. Biol.* **44** 2321-2341

Karlsson M G, Karlsson M and Ma C-M 1999 Treatment head design for multileaf collimated high-energy electrons *Med. Phys.* **26** 2161-2167

Kawrakow I 2000 Accurate condensed history Monte Carlo simulation of electron transport I. EGSnrc, the new EGS4 version *Med. Phys.* **27** 485-98

Kawrakow I and Fippel M 2000 VMC++, a fast MC algorithm for radiation treatment planning In: *Proceedings XIII International Conference on the Use of Computers in Radiation Therapy* Eds. Schlegel W and Bortfeld T (Heidelberg: Springer-Verlag)

Kawrakow I 2001 VMC++, Electron and photon Monte Carlo calculations optimized for radiation treatment planning In: *Advanced Monte Carlo for Radiation Physics, Particle Transport Simulation and Applications: Proceedings of the Monte Carlo 2000 Meeting* Kling A, Barao F, Nakagawa M, Távora L and Vaz P Eds. (Berlin: Springer-Verlag)

Kawrakow I and Rogers D W O 2001 The EGSnrc system, a status report In: *Advanced Monte Carlo for Radiation Physics, Particle Transport Simulation and Applications: Proceedings of the Monte Carlo 2000 Meeting* Kling A, Barao F, Nakagawa M, Távora L and Vaz P Eds. (Berlin: Springer-Verlag)

Kawrakow I and Rogers D W O 2002 The EGSnrc code system: Monte Carlo simulation of electron and photon transport NRCC Report *PIRS-701*

Keall P J and Hoban P W 1996 A Review of electron beam dose calculation algorithms *Aust. Phys. Eng. Sci. Med.* **19** 111-130

Knöös T, Ceberg C, Weber L and Nilsson P 1994 The dosimetric verification of a pencil beam based treatment planning system *Phys. Med. Biol.* **39** 1609-1628

Knöös T, Ahnesjö A, Nilsson P and Weber L 1995 Limitations of a pencil beam approach to photon dose calculations in lung tissue *Phys. Med. Biol.* **40** 1411-1420

Kosunen A, Järvinen H, Vatnitskij S, Ermakov I, Chervjakov A, Kulmala J, Pitkänen M, Väyrynen T and Väänänen A 1993 Inter-comparison of radiotherapy treatment planning systems for external photon and electron beam dose calculations *Radiother. Oncol.* **29** 327-335

Krieger T and Sauer O A 2005 Monte Carlo- versus pencil-beam-/collapsed-cone-dose calculation in a heterogeneous multi-layer phantom *Phys. Med. Biol.* **50** 859-868

Kron T 1999 Dose measuring tools In: The modern technology of radiation oncology Van Dyk J Ed. (Madison WI: Medial Physics Publishing)

Leunens G, Menten J, Weltens C, Verstraete J and van der Schueren E 1993 Quality assessment of medical decision making in radiation oncology: variability in target volume delineation for brain tumours *Radiother. Oncol.* **29** 169-175

Lewis R D, Ryde S J S, Seaby A W, Hancock D A and Evans C J 2000 Use of Monte Carlo computations in benchmarking radiotherapy treatment planning system algorithms *Phys. Med. Biol.* **45** 1755-1764.

Low D A, Harms W B, Mutic S and Purdy J A 1998 A technique for the quantitative evaluation of dose distributions *Med. Phys.* **25** 656-661

Low D A and Dempsey J F 2003 Evaluation of the gamma dose distribution comparison method *Med. Phys.* **30** 2455-2464

Ma C-M and Jiang S B 1999 Monte Carlo modelling of electron beams from medical accelerators *Phys. Med. Biol.* **44** R157-R189

Ma C-M, Mok E, Kapur A, Pawlicki T, Findley D, Brain S, Forster K and Boyer A L 1999 Clinical implementations of a Monte Carlo treatment planning system *Med. Phys.* **26** 2133-2143

Mackie T R, Bielajew A F, Rogers D W O and Battista J J 1988 Generation of photon energy deposition kernels using EGS Monte Carlo code *Phys. Med. Biol.* **33** 1-20

Mackie T R 1990 Applications of the Monte Carlo method in radiotherapy In: The dosimetry of ionizing radiation vol. III Kase K, Bjärngard B and Attix F Eds. (San Diego, CA: Academic Press)

Mackie T R, Reckwerdt P and Papanikolaou N 1995 3-D photon beam dose algorithms In: 3D radiation treatment planning and conformal therapy Purdy J A and Emami B Eds. (Madison, WI: Medial Physics Publishing)

Mackie T R, Kapatoes J, Ruchala K, Lu W, Wu C, Olivera G, Forrest L, Tome W, Welsh J, Jeraj R, Harari P, Reckwerdt P, Paliwal B, Ritter M, Keller H, Fowler J and Mehta M 2003 Image guidance for precise conformal radiotherapy *Int. J. Radiat. Oncol. Biol. Phys.* **56** 89-105

Mageras G S and Yorke E 2004 Deep inspiration breath hold and respiratory gating strategies for reducing organ motion in radiation treatment *Semin. Radiat. Oncol.* **14** 65-75

Mainegra-Hing E, Kawrakow I and Rogers D W O 2003 Calculations for plane-parallel ion chambers in ^{60}Co beams using the EGSnrc Monte Carlo code *Med. Phys.* **30** 179-189

Martens C, Reynaert N, De Wagter C, Nilsson P, Coghe M, Palmans H, Thierens H and De Neve W 2002 Underdosage of the upper-airway mucosa for small fields as used in intensity-modulated radiation therapy: A comparison between radiochromic film measurements, Monte Carlo simulations and collapsed cone convolution calculations *Med. Phys.* **29** 1528-1535

McCaffrey J P, Mainegra-Hing E, Kawrakow I, Shortt K R and Rogers D W O 2004 Evidence for using Monte Carlo calculated wall attenuation and scatter correction factors for three styles of graphite-walled ion chambers *Phys. Med. Biol.* **49** 2491-2501

McCullough E C and Krueger A M 1980 Performance evaluation of computerized treatment planning systems for radiotherapy: external photon beams *Int. J. Radiat. Oncol. Biol. Phys.* **6** 1599-1605

Miften M, Wiesmeyer M, Kapur A and Ma C-M 2001 Comparison of RTP dose distributions in heterogeneous phantoms with the BEAM Monte Carlo simulation system *J. Appl. Clin. Med. Phys.* **2** 21-31

Mijnheer B J, Battermann J J and Wambersie A 1987 What degree of accuracy is required and can be achieved in photon and neutron therapy? *Radiother. Oncol.* **8** 237-252

Mobit P N, Sandison G A and Nahum A E 2000 Electron fluence perturbation correction factors for solid state detectors irradiated in megavoltage electron beams *Phys. Med. Biol.* **45** 255-265

Mohan R 1997 Why Monte Carlo? In: *Proceedings XII International Conference on the Use of Computers in Radiation Therapy* Leavitt D D and Starkschall G Eds. (Madison WI: Medical Physics Publishing)

Mora G, Pawlicki T, Maio A and Ma C-M 2001 Effect of voxel size on Monte Carlo dose calculations for radiotherapy treatment planning In: *Advanced Monte Carlo for Radiation Physics, Particle Transport Simulation and Applications: Proceedings of the Monte Carlo 2000 Meeting* Kling A, Barao F, Nakagawa M, Távora L and Vaz P Eds. (Berlin: Springer-Verlag)

Nahum A E 1996 Perturbation effects in dosimetry: Part I. Kilovoltage x-rays and electrons *Phys. Med. Biol.* **41** 1531-1580

NCS 2005 Netherlands Commission on Radiation Dosimetry, Quality Assurance of 3-D Treatment Planning Systems for external photon and electron beams, In Press

Nelson W R, Hirayama H and Rogers D W O 1985 The EGS4 code system Report SLAC-265 Stanford Linear Accelerator Center, Stanford CA

Nisbet A, Beange I, Vollmar H-S, Irvine C, Morgan A and Thwaites D I 2004 Dosimetric verification of a commercial collapsed cone algorithm in simulated clinical situations *Radiother. Oncol.* **73** 79-88

Northey B J and Zavgorodni S F 2002 Optimisation of electron cone design in high energy radiotherapy using the Monte Carlo method *Aust. Phys. Eng. Sci. Med.* **25** 7-15

Nucletron 2005 Oncentra MasterPlan v. 1.4 Physics reference manual

Paelinck L, Reynaert N, Thierens H, De Neve W and De Wagter C 2005 Experimental verification of lung dose with radiochromic film: comparisons with Monte Carlo simulations and commercially available treatment planning systems *Phys. Med. Biol.* **50** 2055-2069

Palm Å and LoSasso T 2005 Influence of phantom material and phantom size on radiographic film response in therapy photon beams *Med. Phys.* **32** 2434-2441

Paulino A C, Thorstad W L and Fox T 2003 Role of fusion in radiotherapy treatment planning *Semin. Nucl. Med.* **33** 238-243

Popescu I and Bush K 2005 Commissioning of virtual linacs for Monte Carlo simulations by optimizing photon source characteristics *Radiother. Oncol.* **76** (Suppl.2) S43

Rasch C, Steenbakkers R and van Herk M 2005 Target definition in prostate, head, and neck *Semin. Radiat. Oncol.* **15** 136-145

Rikner G 1985 Characteristics of a selectively shielded p-Si detector in a ^{60}Co and 8 and 16 MV roentgen radiation *Acta Radiol. Oncol.* **24** 205-208

Ringborg U, Bergqvist D, Brorsson B, Cavallin-Ståhl E, Ceberg J, Einhorn N, Frödin J-E, Järhult J, Lamnevik G, Lindholm C, Littbrand B, Norlund A, Nylén U, Rosén M, Svensson H and Möller T R 2003 The Swedish council on technology assessment in health care (SBU) systematic overview of radiotherapy for cancer including a prospective survey of radiotherapy practice in Sweden 2001 - summary and conclusions *Acta Oncol.* **42** 357-365

Roberts R 2001 How accurate is a CT-based dose calculation on a pencil beam TPS for a patient with a metallic prosthesis? *Phys. Med. Biol.* **46** N227-N234

Rogers D W O and Bielajew A F 1990 Monte Carlo techniques of electron and photon transport for radiation dosimetry In: The dosimetry of ionizing radiation vol. III Kase K, Bjärngard B and Attix F Eds. (San Diego, CA : Academic Press)

Rogers D W O, Faddegon B A, Ding G X, Ma C-M, We J and Mackie T R 1995 BEAM: A Monte Carlo code to simulate radiotherapy treatment units *Med. Phys.* **22** 503-524

Rogers D W O and Treurniet J 1999 Monte Carlo calculated wall and axial non-uniformity corrections for primary standards of air kerma NRCC Report *PIRS-663*

Rogers D W O, Ma C-M, Walters B, Ding G X, Sheikh-Bagheri D and Zhang G 2002 BEAMnrc Users Manual NRCC Report *PIRS-0509A (rev G)*

Rogers D W O 2002 Monte Carlo techniques in radiotherapy *Phys. in Canada* **58** 63-70

SGSMP 1997 Swiss Society of Radiobiology and Medical Physics, Quality control of treatment planning systems for teletherapy, Recommendations no. 7

Shiu A S, Tung S, Hogstrom K R, Wong J W, Gerber R L, Harms W B, Purdy J A, Ten Haken R K, McShan D L and Fraass B A 1992 Verification data for electron beam dose algorithms *Med. Phys.* **19** 623-636

Spezi E, Lewis D G and Smith C W 2002 A DICOM-RT-based toolbox for the evaluation and verification of radiotherapy plans *Phys. Med. Biol.* **47** 4223-4232

Spezi E 2003 A Monte Carlo investigation of the accuracy of intensity modulated radiotherapy PhD Thesis University of Wales

Stock M, Kroupa B and Georg D 2005 Interpretation and evaluation of the γ index and the γ index angle for verification of IMRT hybrid plans *Phys. Med. Biol.* **50** 399-411

Traneus E, Ahnesjö A, Fippel M, Kawrakow I, Nüsslin F, Zeng G and Åsell M 2001 Application and verification of a coupled multi-source electron beam source model for Monte Carlo based treatment planning *Radiother. Oncol.* **61** (Suppl.1) S102

Van Dyk J, Barnett R B, Cygler J E and Shragge P C 1993 Commissioning and quality assurance of treatment planning computers *Int. J. Radiat. Oncol. Biol. Phys.* **26** 261-273

van't Veld A A 1997 Analysis of accuracy in dose and position in calculations of a treatment planning system for blocked photon fields *Radiother. Oncol.* **45** 245-251

Venselaar J, Welleweerd H and Mijnheer B 2001 Tolerances for the accuracy of photon beam dose calculations of treatment planning systems *Radiother. Oncol.* **60** 191-201

Venselaar J and Welleweerd H Application of a test package in an inter-comparison of the photon dose calculation performance of treatment planning systems used in a clinical setting *Radiother. Oncol.* **60** 203-213

Verhaegen F 2002 Evaluation of the EGSnrc Monte Carlo code for interface dosimetry near high-Z media exposed to kilovolt and ^{60}Co photons *Phys. Med. Biol.* **47** 1691-1705

Verhaegen F and Seuntjens J 2003 Monte Carlo modelling of external radiotherapy photon beams *Phys. Med. Biol.* **48** R107-R164

Walters B R B and Rogers D W O 2002 DOSXYZnrc Users Manual NRCC Report *PIRS-794*

Wambersie A 2001 What accuracy is required and can be achieved in radiation therapy? *Radiochim. Acta* **89** 255-264

Wang L, Yorke E and Chui C-S 2001 Monte Carlo evaluation of tissue inhomogeneity effects in the treatment of the head and neck *Int. J. Radiat. Oncol. Biol. Phys.* **50** 1339-1349

Webb S 2005 Contemporary IMRT developing physics and clinical implementation (London: Institute of Physics Publishing)

Weber L and Nilsson P 2002 Verification of dose calculations with a clinical treatment planning system based on a point kernel does engine *J. Appl. Clin. Med. Phys.* **3** 73-87

Welleweerd J and van der Zee W 1998 Dose calculation for asymmetric fields using Plato version 2.01 *Radiother. Oncol.* **48** (Suppl.1) S134

Wieslander E, Sheikh-Bagheri D, Weber L, Ahnesjö A and Knöös T 2001 Monte Carlo verification of a multi-source model used in a treatment planning system *Radiother. Oncol.* **61** (Suppl.1) S101

Ye S-J, Pareek P N, Spencer S, Duan J and Brezovich I A 2005 Monte Carlo techniques for scattering foil design and dosimetry in total skin electron irradiations *Med. Phys.* **32** 1460-1468

Yorke E D, Wang L, Rosenzweig K E, Mah D, Paoli J-B and Chui C-S 2002 Evaluation of deep inspiration breath-hold lung treatment plans with Monte Carlo dose calculation *Int. J. Radiat. Oncol. Biol. Phys.* **53** 1058-1070

Populärvetenskaplig sammanfattning

För många cancerpatienter är strålbehandling ett viktigt behandlingsalternativ. En framgångsrik behandling kräver att den absorberade dosen till patienten kan ges med stor noggrannhet. Detta eftersom en liten avvikelse i absorberad dos kan påverka behandlingens resultat. Strålbehandling sker idag med avancerad teknik och utrustning där osäkerheterna i varje led i behandlingskedjan måste minimeras.

Ett led i förberedelserna är att beräkna den absorberade dosen till patienten. Detta görs idag med avancerade datorprogram, så kallade dosplaneringssystem. Noggrannheten i den beräknade dosen har vanligtvis studerats med experimentella mätningar. Experimentella data begränsas av vad som är praktiskt genomförbart och kan vara förenade med osäkerheter, som är relaterade till mätutrustningen. Behandlingsapparatens stabilitet i tiden påverkar också resultaten, då det kan ta dagar att samla in all den information som behövs.

I detta arbete har möjligheten och fördelarna med att använda en Monte Carlo-metod för att utvärdera noggrannheten i dosplaneringssystemens dosberäkning studerats. Monte Carlo är en sannolikhetsbaserad beräkningsmetod, som utgår från grundläggande fysikaliska egenskaper. En modell av en behandlingsapparat, en s.k. virtuell behandlingsapparat, har konstruerats i ett Monte Carlo-baserat datorprogram. Denna virtuella behandlingsapparat har använts för att bland annat generera information motsvarande den man kan mäta upp för kliniska behandlingsapparater. Den virtuella behandlingsapparaten har lagts in i dosplaneringssystemet på samma sätt som kliniska behandlings-apparater. Jämförelser mellan den virtuella behandlingsapparaten (Monte Carlo-simuleringar) och dess motsvarighet i dosplaneringssystemet kan användas för att studera noggrannheten i den beräknade dosfördelningen i olika situationer. Denna virtuella behandlingsapparat kan också användas för att studera hur väl dosplaneringssytemet kan beskriva de strålfält som genereras av behandlings-apparaten.

Resultaten visar att konceptet med den virtuella behandlingsapparaten framgångsrikt kan användas för att studera noggrannheten i dosplanerings-systems dosberäkning. Fördelarna med detta koncept har också illustrerats i flera situationer, där motsvarande jämförelser baserade på mätningar är begränsade eller till och med omöjliga. Till exempel har noggrannheten i dosberäkningen för några vanliga patientbehandlingar studerats.

Konceptet med den virtuella behandlingsapparaten gör det möjligt att i detalj studera de modeller som beskriver strålfälten och den efterföljande beräkningen av dosfördelningen i patienten. Den virtuella behandlings-apparaten är därför ett värdefullt verktyg för både användare och tillverkare.